

Transcriptional signatures modulating shoot apical meristem morphometric and plant architectural traits enhance yield and productivity in chickpea

Laxmi Narnoliya¹, Udit Basu¹, Deepak Bajaj¹, Naveen Malik¹, Virevol Thakro¹, Anurag Daware¹, Akash Sharma¹, Shailesh Tripathi², Venkatraman S. Hegde², Hari D. Upadhyaya³, Ashok K. Singh², Akhilesh K. Tyagi^{1,4} and Swarup K. Parida^{1,*} 

¹Genomics-assisted Breeding and Crop Improvement Laboratory, National Institute of Plant Genome Research (NIPGR), Aruna Asaf Ali Marg, New Delhi 110067, India,

²Division of Genetics, Indian Agricultural Research Institute (IARI), New Delhi 110012, India,

³International Crops Research Institute for the SemiArid Tropics (ICRISAT), Patancheru, Telangana 502324, India, and

⁴Department of Plant Molecular Biology, University of Delhi, South Campus, New Delhi 110021, India

Received 11 September 2018; revised 31 January 2019; accepted 7 February 2019; published online 11 February 2019.

*For correspondence (e-mails swarup@nipgr.ac.in; swarupdbt@gmail.com).

SUMMARY

Plant height (PH) and plant width (PW), two of the major plant architectural traits determining the yield and productivity of a crop, are defined by diverse morphometric characteristics of the shoot apical meristem (SAM). The identification of potential molecular tags from a single gene that simultaneously modulates these plant/SAM architectural traits is therefore prerequisite to achieve enhanced yield and productivity in crop plants, including chickpea. Large-scale multienvironment phenotyping of the association panel and mapping population have ascertained the efficacy of three vital SAM morphometric trait parameters, SAM width, SAM height and SAM area, as key indicators to unravel the genetic basis of the wide PW and PH trait variations observed in *desi* chickpea. This study integrated a genome-wide association study (GWAS); quantitative trait locus (QTL)/fine-mapping and map-based cloning with molecular haplotyping; transcript profiling; and protein-DNA interaction assays for the dissection of plant architectural traits in chickpea. These exertions delineated natural alleles and superior haplotypes from a *CabHLH121* transcription factor (TF) gene within the major QTL governing PW, PH and SAM morphometric traits. A genome-wide protein-DNA interaction assay assured the direct binding of a known stem cell master regulator, *CaWUS*, to the *WOX*-homeodomain TF binding sites of a *CabHLH121* gene and its constituted haplotypes. The differential expression of *CaWUS* and transcriptional regulation of its target *CabHLH121* gene/haplotypes were apparent, suggesting their collective role in altering SAM morphometric characteristics and plant architectural traits in the contrasting near isogenic lines (NILs). The NILs introgressed with a superior haplotype of a *CabHLH121* exhibited optimal PW and desirable PH as well as enhanced yield and productivity without compromising any component of agronomic performance. These molecular signatures of the *CabHLH121* TF gene have the potential to regulate both PW and PH traits through the modulation of proliferation, differentiation and maintenance of the meristematic stem cell population in the SAM; therefore, these signatures will be useful in the translational genomic study of chickpea genetic enhancement. The restructured cultivars with desirable PH (semidwarf) and PW will ensure maximal planting density in a specified cultivable field area, thereby enhancing the overall yield and productivity of chickpea. This can essentially facilitate the achievement of better remunerative outputs by farmers with rational land use, therefore ensuring global food security in the present scenario of an increasing population density and shrinking per capita land area.

Keywords: chickpea, *desi*, fine mapping, genome-wide association study, *kabuli*, map-based cloning, near isogenic lines, plant height, plant width, productivity, quantitative trait locus, RIL, shoot apical meristem, single nucleotide polymorphisms, transcription factor, yield.

INTRODUCTION

Plant architecture is the three-dimensional organization of the plant body and is represented by various major component traits such as the inflorescence architecture, plant height (PH), plant width (PW), branching pattern, and others. The plant architecture determines the ultimate agronomic value of a crop by influencing its photosynthetic efficiency and maturity time, and therefore overall crop growth, development and production. In the present scenario of unforeseen climate change and diminishing cultivable land area, the development and use of proficient strategies for enhancing crop yield is essential to ensure global food security. Ever since the advent of the Green Revolution in the 1940s, the manipulation of plant architecture has clearly arisen as an efficient strategy to enhance crop yield and productivity within land and climatic constraints. In this regard, significant accomplishments have been achieved with the development of lodging-resistant semidwarf varieties of wheat and rice by introducing the genes/alleles that control one of the vital plant architecture traits, PH, leading to enhanced grain yield in these staple food crops (Peng *et al.*, 1999; Evenson and Gollin, 2003). An ideal plant architecture also contributes to the adaptation of crops towards different environmental stress along with enhancing their photosynthetic efficiency, yield, and harvest index (Reinhardt and Kuhlemeier, 2002; Sakamoto *et al.*, 2004; Yang and Hwa, 2008). Plant width is another vital plant architectural trait that has a direct impact on the efficient use of land area under cultivation. With limiting land resources, optimizing PW without compromising yield per plant will accommodate a greater number of plants in a specified cultivable land area and thereby significantly enhance the crop yield and productivity.

Manipulation of plant architecture requires a comprehensive understanding of the genetic networks and regulatory pathways governing its various major contributing traits in crops (Pickersgill, 2007; Jin *et al.*, 2008). Deciphering the genetic and molecular mechanism that underlies plant architecture variation will not only address the basic fundamental intricacies but also facilitate genomics-assisted breeding to develop high-yielding cultivars restructured with an ideal plant type (Wang and Li, 2008). The gene regulatory networks within the meristematic cells play a major role in defining the plant architecture. The shoot apical meristem (SAM) is the key organizing centre of stem cells and controls most developmental traits contributing to seed yield in crop plants. It comprises a dome of pluripotent cells that ultimately generates all the organs of the plant shoot and performs the dual functions of organogenesis and stem cell maintenance (Barton, 2010; Thompson *et al.*, 2014, 2015). SAM morphology, a quantitative trait defined by the descriptive measurements of SAM shape and size, can be exploited as target traits for

the genetic enhancement of crop plants. Henceforth, the phenotypic variations of said SAM morphometric characteristics are correlated with allelic diversity scanned from natural and mapping populations through genetic and association mapping to successfully identify potential genomic loci governing diverse plant architectural traits in major food crops (Thompson *et al.*, 2014, 2015; Leiboff *et al.*, 2015; Cai *et al.*, 2016; Saxena *et al.*, 2017). These studies evidently suggest that comprehensive genetic dissection of SAM morphometric and ideal plant architectural traits is vital for crop improvement. This will essentially therefore lay the foundation for designing efficient genomics-assisted breeding strategies to improve yield and productivity in crop plants.

Chickpea (*Cicer arietinum* L.) is a vital nutrient-rich diploid legume crop with a genome size of ~740 Mbp (Kumar *et al.*, 2011; Varshney *et al.*, 2013a). The genome sequences of cultivated *desi* and *kabuli* chickpea and their close wild progenitor *C. reticulatum* have been decoded in the recent past (Jain *et al.*, 2013; Varshney *et al.*, 2013b; Parween *et al.*, 2015; Gupta *et al.*, 2016). These reference genomic resources efficiently facilitate discovery and high-throughput genotyping of sequence-based markers including simple sequence repeats (SSRs) and single nucleotide polymorphisms (SNPs) among the large-scale germplasm accessions (association panel) and mapping populations of chickpea. These exertions drive genome-wide association studies (GWAS) and quantitative trait locus (QTL) mapping that detected several major QTLs and genes governing multiple yield-contributing traits in chickpea (Saxena *et al.*, 2014a; Bajaj *et al.*, 2015a,b; Kujur *et al.*, 2015a,b, 2016; Upadhyaya *et al.*, 2015). Most of these genomics-assisted breeding efforts employed to date in trait dissection for chickpea genetic enhancement are intended to improve the yield per plant. Unfortunately, genetic manipulation of plant architectural traits has yet not been explored for genetic enhancement of this crop legume to increase its yield and productivity.

Chickpea plants are well known for their non-synchronized spreading to semispreading/semierect growth habits, which usually increase the PW and therefore require more space for suitable growth and development. As a consequence, fewer plants can be accommodated in a definite cultivable land area, resulting in low chickpea productivity. In this context, the optimization of PW in addition to PH is essential for the development of lodging-resistant semidwarf plant type chickpea cultivars. Restructured plants with an ideal architecture will enhance the yield and productivity of chickpea and therefore can be useful in providing higher remuneration, especially to small and marginal farmers with minimal land resources. Delineation of functionally relevant genes and alleles governing both SAM morphometric characteristics as well as plant architectural

traits (PH and PW) using diverse integrated genomic strategy is therefore essential. These delineated molecular tags can further be deployed in marker-aided selection for restructuring desirable new plant types, which will be useful to enhance yield and productivity in chickpea.

Keeping that in mind, the current investigation integrated diverse molecular genetics approaches with genomics-assisted breeding and functional genomic strategies to decode the complex genetic architecture of vital SAM morphometric trait characteristics as well as two major plant architectural traits in chickpea, PW and PH. The GWAS, regional association analysis, QTL/fine-mapping and map-based cloning were correlated with gene haplotype-specific association and transcript profiling and the protein–DNA interaction assay in the constituted association panel (*desi* and *kabuli* germplasm accessions), as well as recombinant inbred lines (RIL) and NIL mapping populations of chickpea with contrasting plant and SAM architectural traits. This result assisted us in delineating the most promising molecular signatures (genes, natural alleles, and superior haplotypes) regulating vital plant architectural traits, PW and PH through the modulation of SAM morphometric features, with an aim to drive high yield and productivity in chickpea.

RESULTS

Phenotypic evaluation and characterization of an association panel for major plant architectural and SAM morphometric traits in chickpea

An association panel comprising 291, including 189 *desi* and 102 *kabuli*, germplasm accessions was employed for genetic dissection of major plant and SAM architectural traits through GWAS in chickpea (Table S1). The multi-environment (field and controlled conditions) replicated phenotypic evaluation and characterization of the association panel were performed for two vital plant architectural traits, PW and PH, and seven SAM morphometric trait parameters, including SAM width (SWi), SAM height (SH), SAM midpoint width (SMWi), SAM height/width ratio (SH/SWi), SAM arc length (SAL), SAM area (SA) and SAM radius (SR), based on histology (Figure 1). A comprehensive *desi* and *kabuli* cultivar-wise analysis exhibited the wider level of phenotypic variation for five of these major architectural traits (PW, PH, SWi, SH, and SA) among *desi* accessions (6.08–23.35% coefficient of variation (CV)) compared with that among *kabuli* accessions (1.69–9.27% CV). A greater degree of phenotypic variation was observed for the SH (23.35% CV) followed by the SA (19.84%) and PH (11.74%) traits among 189 *desi* accessions (Table S2 and Figure 2a, b). In *kabuli*, phenotypic variation was maximum for the PH (9.03% CV) followed by the PW (6.38%) and SA (3.20%) traits among 102 accessions. The normal frequency distribution was evident, particularly for the PW

and PH traits phenotyped in the multi-environment field conditions among 291 *desi* and *kabuli* accessions (Figure 2a). The high broad-sense heritability (H^2) of the PW, PH, SWi, SH, and SA traits (75–83%) among the *desi* and *kabuli* accessions was apparent. A detailed correlation analysis and subsequent hierarchical cluster display of the studied SAM morphometric and plant architectural traits were performed among 291 *desi* and *kabuli* accessions. A significant positive correlation (65–73%) among PW, PH, SWi, and SH traits in all these *desi* and *kabuli* accessions was evident (Figures 1d and 2c). Comparatively, a high correlation (91–93%) among these plant architectural and SAM morphometric traits in 189 accessions of *desi* chickpea was observed.

GWAS and regional association analysis scans of potential genomic loci associated with major plant architectural and SAM morphometric traits in chickpea

Genome-wide association study was performed to identify the potential genomic loci associated with two vital plant architectural traits (PW and PH) and three major SAM morphometric traits (SWi, SH and SA) in chickpea. Primarily, high-throughput genotyping of SNPs mined by resequencing of 291 *desi* and *kabuli* accessions representing an association panel was carried out using a genotyping-by-sequencing (GBS) assay. Overall, this procedure detected 333 001 high-quality SNPs with an average frequency of 625.6 SNPs per Mb (Table S3). Detailed structural annotation of SNPs in diverse coding and non-coding sequence components of the genome/genes are depicted in Figure S1 and described briefly in Data S1. The molecular diversity and genetic relatedness analysis based on the unrooted phylogenetic tree, population structure and principal component analysis (PCA) differentiated all 291 accessions from each other and overall grouped these accessions into two distinct population groups, POP I and POP II (Figure S2a–c). The linkage disequilibrium (LD) estimate in an association panel illustrated an overall LD decay (r^2 reduced to half of its maximum value) nearly at a 150-kb physical distance of the chickpea chromosomes (Figure S2d).

For GWAS, high-throughput genotyping data for the 333 001 SNPs assayed in 291 *desi* and *kabuli* accessions (association panel) were correlated with their molecular diversity, population genetic structure and PCA information, as well as the multi-environment (field/controlled condition) replicated phenotyping data for the PW, PH, SWi, SH, and SA traits. GWAS at a false discovery rate (FDR) cut-off ≤ 0.05 using multiple statistical methods of association mapping detected six SNP loci that showed a significant association with the PW, PH, SWi, SH, and SA traits at $P \leq 10^{-8}$ (Table 1 and Figure 3a). All six trait-associated SNPs were well validated by a general linear model (GLM) and a mixed linear model (MLM) of TASSEL as well as a compressed mixed linear model (CMLM), population parameters previously

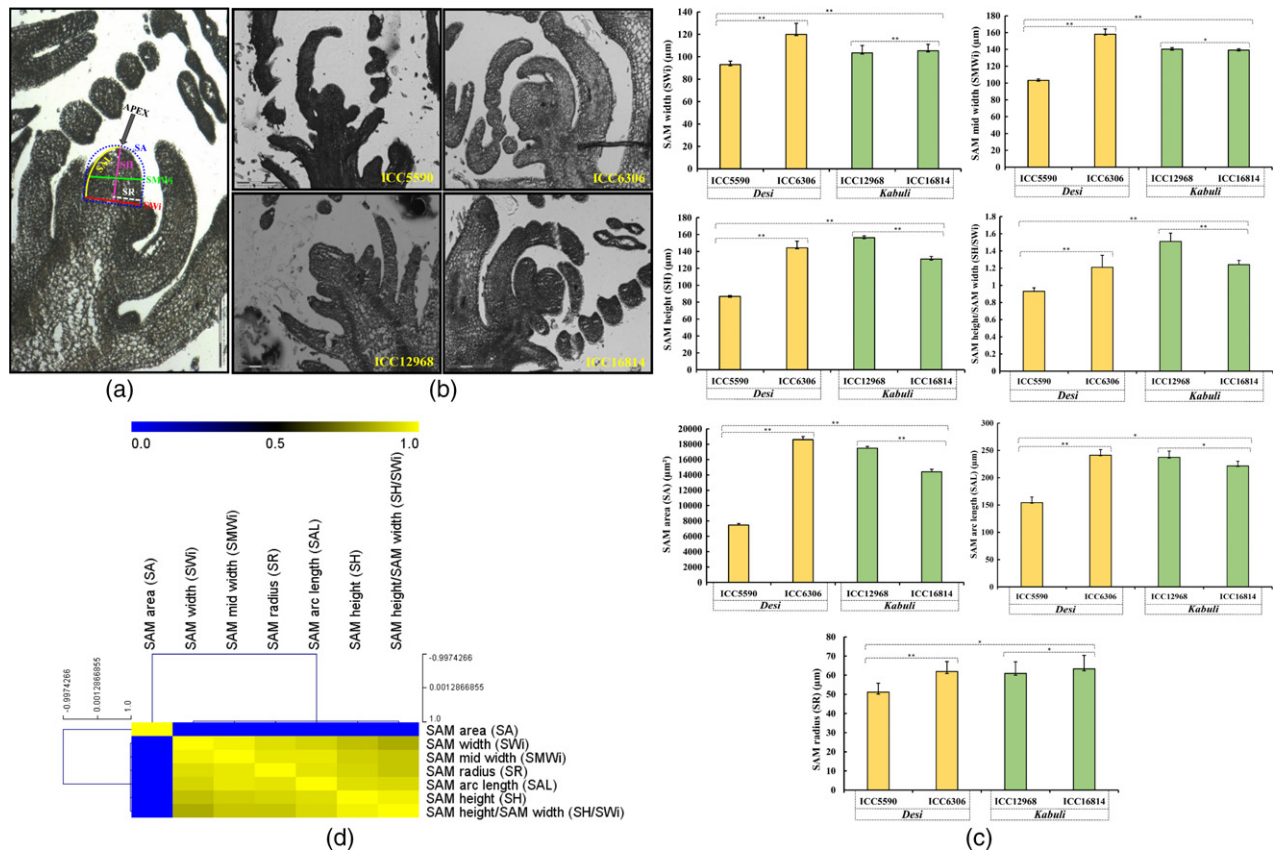


Figure 1. SAM morphometric trait variation among *desi* and *kabuli* chickpea accessions.

(a) SAM architecture of a chickpea accession examined based on its seven major morphometric trait parameters (SWi, SMWi, SH, SH/SWi, SA, SAL, and SR) using a histological assay.

(b) Histology of four *desi* (ICC 5590 and ICC 6306) and *kabuli* (ICC 12968 and ICC 16814) accessions in accordance with the indicated major morphometric trait parameters, showing their markedly varied SAM architecture.

(c) Bar diagrams depicting the measurement of seven major SAM morphometric trait parameters (SWi, SMWi, SH, SH/SWi, SA, SAL, and SR) between two accessions representing each *desi* (ICC 5590 and ICC 6306) and *kabuli* (ICC 12968 and ICC 16814) chickpea. Dotted lines represent variations among four *desi* and *kabuli* accessions as well as between two accessions each belonging to *desi* (yellow) and *kabuli* (green). Significance at * $P < 0.05$ (pair-wise t -test) and ** $P < 0.01$ (pair-wise t -test).

(d) A hierarchical cluster display depicting the phenotypic correlation among SAM morphometric traits in the accessions, especially those representing *desi* chickpea. The average Pearson's correlation value estimated among the studied traits represented at the top with a colour scale; blue, dark blue and yellow denote a low, medium and high levels of correlation, respectively. Digits indicated in the vertical and horizontal bars illustrate the range (minimum, optimum and maximum) of the correlation coefficient measured among traits.

determined (P3D) and efficient mixed model association eXpedited (EMMAX) strategies of Genome Association and Prediction Integrated Tool (GAPIT). Of these, the CMLM strategy of GAPIT taking into account population structure and principal components as well as ancestry were found to be the best model for GWAS of plant architectural and SAM morphometric traits in chickpea. These associated SNPs were physically mapped on three chromosomes (*Ca4*, *Ca6*, and *Ca8*) (Table 1 and Figure 3a). Five of six trait-associated SNP loci derived from the diverse coding sequence components of five genes exhibited non-synonymous amino acid substitutions. The remaining one associated SNP was detected in the intergenic region of the chickpea genome. The phenotypic variation explained (PVE) for the studied plant and SAM architectural traits by six significant SNPs in a constituted association panel varied from 15 to 34% R^2

(Table 1). Compared with five other trait-associated SNPs, a coding SNP (G/A) showing a non-synonymous amino acid substitution (Arginine: CGT to histidine: CAT) in a basic helix–loop–helix (*bHLH*) transcription factor (TF) gene exhibited a strong association (10^{-9} P with 34% combined PVE) with the PW, PH, SWi, SH, and SA traits (Table 1 and Figure 3a). This identified *bHLH* TF gene was further classified as '*CabHLH121*' with a Myc-type functional domain, in accordance with the comprehensive genome-wide identification of 135 *bHLH* TF-encoding genes annotated from the *kabuli* chickpea genome. Therefore, a strong plant architectural (PW and PH) and SAM morphometric (SWi, SH, and SA) trait-associated SNP detected in a *CabHLH121* TF gene employing high-resolution GWAS was considered a promising candidate to drive genomics-assisted breeding and crop improvement of chickpea.

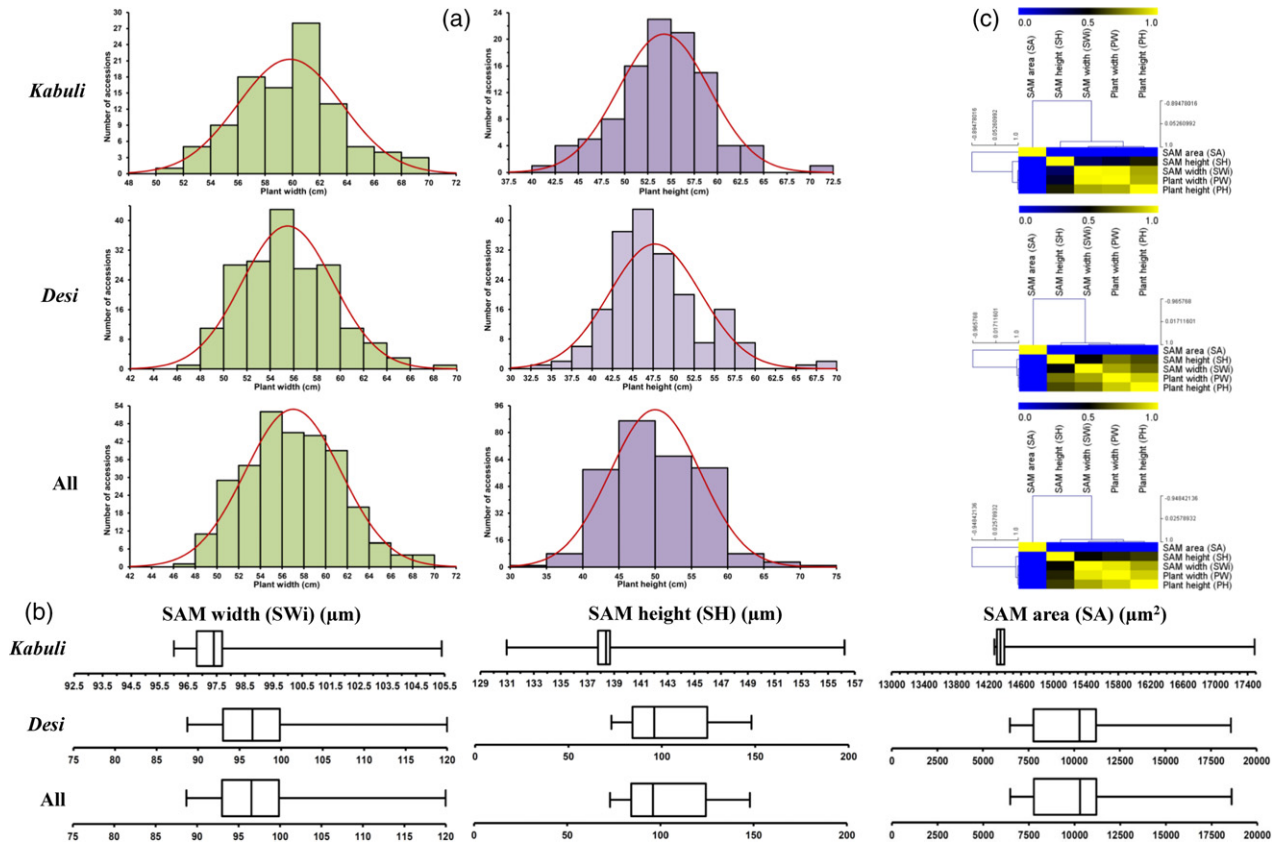


Figure 2. Phenotypic variation of major SAM morphometric and plant architectural traits in a constituted association panel. (a) Frequency distribution of two major plant architectural traits, plant width (PW) and plant height (PH) variation, estimated among all 291, including 189 *desi* and 102 *kabuli*, accessions. (b) Boxplots depicting the phenotypic variation among three major SAM morphometric trait parameters, SWi, SH and SA, among all 291, including 189 *desi* and 102 *kabuli*, accessions. Box edges represent the upper and lower quantiles, with median values shown in the middle of the box. (c) A hierarchical cluster display depicting the phenotypic correlation among plant architectural (PW and PH) and SAM morphometric (SWi, SH and SA) traits in all 291, including 189 *desi* and 102 *kabuli*, accessions. The average Pearson's correlation value measured among the studied traits is represented at the top with a colour scale; blue, dark blue and yellow denote a low, medium and high levels of correlation, respectively. Digits indicated in the vertical and horizontal bars illustrate the range (minimum, optimum and maximum) of correlation coefficient estimated among traits.

To further assure the association potential of GWAS-derived genomic SNP loci in governing PW, PH, SWi, SH, and SA traits of chickpea, a gene-by-gene regional association analysis was performed. For this process, high-resolution targeted resequencing at the most 150-kb genomic regions (exhibiting significant LD decay) flanking six GWAS-derived trait-associated SNPs was performed in 291 *desi* and *kabuli* accessions (association panel). The genotyping data for the SNPs from these target intervals of associated genomic loci were integrated with the multi-environment (field/controlled condition) phenotyping data of five studied plant and SAM architectural traits among accessions belonging to an association panel. This procedure delineated a shortest 0.14-Mb genomic interval (0.25–0.39 Mb with 16 genes) of significant LD resolution (mean $r^2 = 0.86$) covering either side of a GWAS-derived non-synonymous coding SNP (*CaKSNP3493*(G/A) at 0.28 Mb) in a *CabHLH121* TF gene, which was strongly associated with the PW, PH, SWi, SH, and SA traits (Figure 3b). This

finding infers the added-advantage of combining GWAS and regional association analysis to scale-down a significant trait-associated longer LD-block with many candidate genes into a functionally relevant real causal gene, which has been well demonstrated in multiple crop plants (Yano *et al.*, 2016).

Genetic mapping of major QTL ascertains the strong association potential of *CabHLH121* TF gene for major plant architectural and SAM morphometric traits in chickpea

Two accessions representing each *desi* (ICC 5590 and ICC 6306) and *kabuli* (ICC 12968 and ICC 16814) were selected from the constituted association panel based on their contrasting PH and PW traits, as well as SAM morphometric trait characteristics, for genetic mapping of major QTLs governing plant and SAM architectural traits in chickpea (Figure 1a,b). In *desi* chickpea, accession ICC 6306 with broad PW and tall PH exhibited significantly higher trait

Table 1 SNPs significantly associated with major plant architectural and SAM morphometric traits in chickpea

SNP IDs	SNP physical positions (bp)		Kabuli chromosomes	Gene accession IDs	Gene identities	Structural annotation	P	Combined PVE ($R^2\%$)	Associated traits
	(C/G)	(A/G)							
CakSNP1340	4 452 380		Ca_Kabuli_Chr04	-	-	Intergenic	1.9×10^{-8}	21	PW, SWi and SA
CakSNP1442	11 231 137		Ca_Kabuli_Chr04	Ca_04355	Major intrinsic protein	Non-synonymous (CDS)	2.5×10^{-8}	19	PW, PH, SWi, SH and SA
CakSNP1506	13 787 720		Ca_Kabuli_Chr04	Ca_04603	Copper amine oxidase	Non-synonymous (CDS)	2.3×10^{-8}	23	PW, PH, SWi, SH and SA
CakSNP1512	13 841 340		Ca_Kabuli_Chr04	Ca_04608	Unknown expressed protein	Non-synonymous (CDS)	2.0×10^{-7}	15	PH, SH and SA
CakSNP2989	57 382 220		Ca_Kabuli_Chr06	Ca_13705	Zinc finger, RING-type	Non-synonymous (CDS)	3.1×10^{-8}	17	PW, SWi and SA
CakSNP3493	281 622		Ca_Kabuli_Chr08	Ca_11909	Basic helix-loop-helix (bHLH)	Non-synonymous (CDS)	1.0×10^{-9}	34	PW, PH, SWi, SH and SA

SNPs, single nucleotide polymorphisms; SAM, shoot apical meristem; PVE, phenotypic variation explained; PW, plant width; PH, plant height; SWi, SAM width; SH, SAM height; SA, SAM area.

values of major SAM morphometric trait parameters, including SWi, SH, SMWi, SH/SWi, SAL, SA, and SR, compared with those estimated in another narrow PW and dwarf PH accession, ICC 5590 (Figure 1a–c). In *kabuli* chickpea, we could not observe any such significant variation in SAM morphometric features other than SH, SH/SWi, and SA (Figure 1c). The phenotypic trait diversity/correlation observed among these four analysed *desi* and *kabuli* accessions, including an association panel (291 accessions), revealed a high significantly positive correspondence between SAM morphometric and plant architectural traits in *desi* chickpea. Therefore, two contrasting *desi* accessions (ICC 5590 and ICC 6306) were selected to develop a *desi* RIL mapping population (ICC 5590 \times ICC 6306), which was utilized further to construct a genetic linkage map and QTL mapping in chickpea.

Primarily, a *desi* genetic linkage map (ICC 5590 \times ICC 6306) was constructed by integrating 9320 genome-wide SNPs across eight chromosomes of chickpea. This generated a genetic map covering a total map length of 1085.98 cM with a map density (mean inter-marker distance) of 0.12 cM (Tables S4 and S5 and Figure S3). Chromosomes 4 and 2 had the highest and lowest saturated genetic maps with map densities of 0.08 and 0.17 cM, respectively. Therefore, a high-resolution genetic linkage map can be efficiently utilized as a reference for molecular mapping of major QTLs governing vital agronomic traits in chickpea. The comprehensive multi-environment (field and controlled conditions) replicated phenotyping of a RIL mapping population (ICC 5590 \times ICC 6306) exhibited a wider level of phenotypic variation (6.62–13.83% CV) and high H^2 (76–82%) for two major plant architectural traits (PW and PH), as well as three vital SAM morphometric traits (SWi, SH and SA), among 278 mapping individuals and parental accessions (Table S2 and Figure S4). Notably, one of the RIL mapping parental *desi* accessions, ICC 5590, exhibited a narrow PW (50.58 cm)/SWi (93 μm) and a low SA (7476.81 μm^2), with a dwarf PH (38.03 cm)/SH (86.78 μm). Another RIL mapping parental *desi* accession, ICC 6306, had a broad PW (68.07 cm)/SWi (119.99 μm) and high SA (18 595.91 μm^2), with a tall PH (66.34 cm)/SH (144.28 μm). The normal frequency distribution and the bi-directional transgressive segregation of the PW, PH, SWi, SH, and SA traits were evident in a RIL mapping population (Figure S4). The detailed correlation analysis and subsequent hierarchical cluster display depicted a positive correlation of 81% among these plant and SAM architectural traits in a RIL population (Figure S5).

For molecular mapping of major QTLs, the genotyping data of 9320 SNPs genetically mapped on chromosomes were correlated with the multi-environment replicated phenotyping information for PW, PH, SWi, SH and SA traits among RIL mapping individuals and parental accessions.

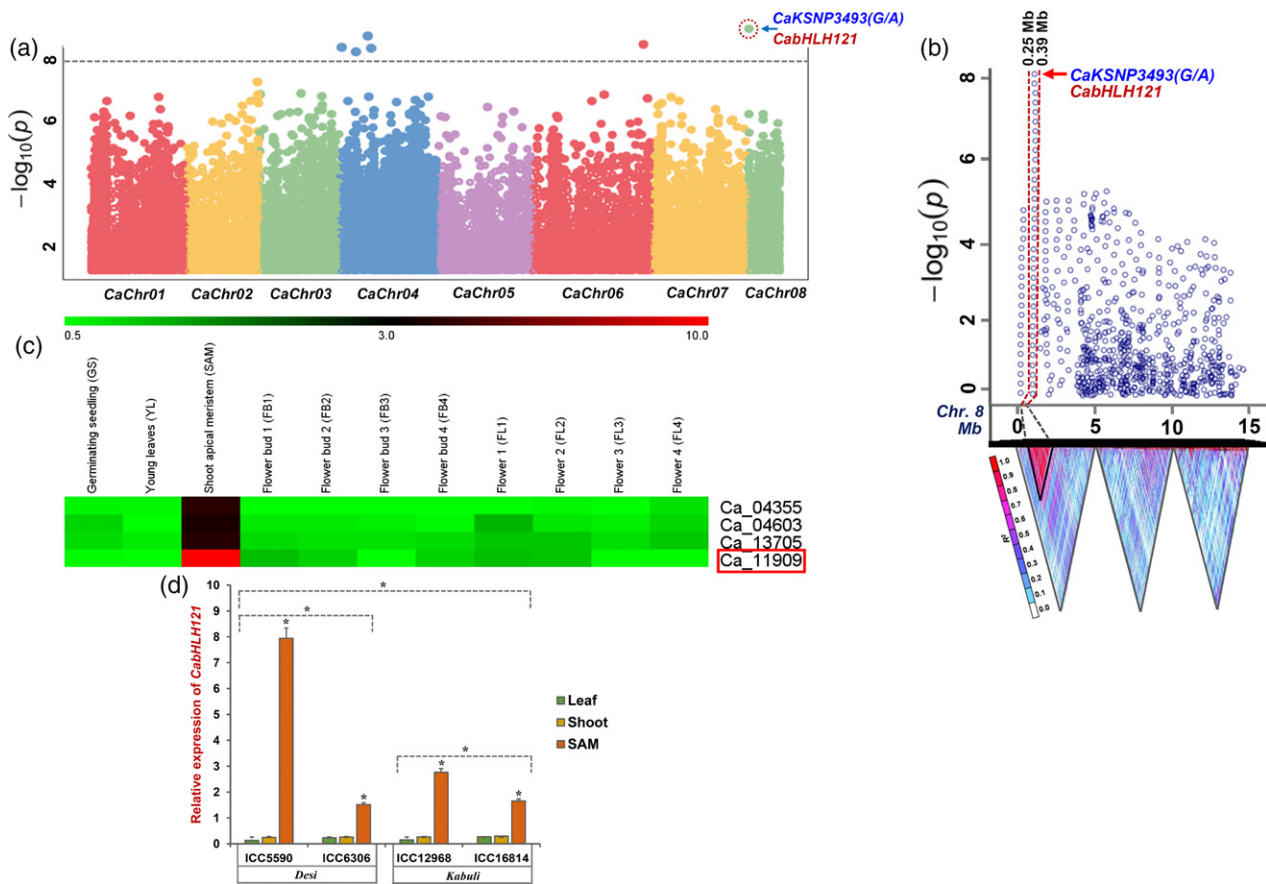


Figure 3. CabHLH121 strongly associated with five major plant and SAM architectural traits expresses specifically in the SAM tissue. (a) GWAS-derived Manhattan plot showing significant *P*-values associated with five major plant architectural (PW and PH) and SAM morphometric (SWi, SH, and SA) traits, obtained using the genome-wide SNPs mined from 291 *desi* and *kabuli* germplasm accessions of chickpea. The *x*-axis represents the relative density of SNPs that physically mapped on eight chromosomes and unanchored scaffolds of the *kabuli* chickpea genome. The *y*-axis indicates the $-\log_{10}(P)$ -value for significant association of SNPs with the studied plant architectural and SAM morphometric traits. Six SNPs exhibiting significant association with traits at cut-off of $P \leq 1 \times 10^{-8}$ are marked with dotted lines. (b) Regional association analysis-led high-resolution LD heat map covering a 0.14-Mb (0.25–0.39 Mb) genomic interval (highlighted with red dotted lines) surrounding a GWAS-derived non-synonymous (arginine: CGT to histidine: CAT) coding SNP (CaKSNP3493 (G/A) at 0.28 Mb) on chromosome 8 exhibited a strong association with plant architectural (PW and PH) and SAM morphometric (SWi, SH and SA) parameters. The arrow specifies the genomic position (bp) of the trait-associated SNP on chromosome 8. In a LD heat map, r^2 indicates the frequency correlation among a pair of alleles across a pair of SNP loci. (c) MultiExperiment Viewer (MeV) illustrating the differential expression profiles of four significant plant and SAM architectural trait-associated genes in diverse tissues, including germinating seedling (GS), young leaf (YL), and shoot apical meristem (SAM) as well as eight flower development stages (FB1, FB2, FB3, FB4, FL1, FL2, FL3, and FL4) of *desi* chickpea accession ICC 4958. The average log signal expression values of genes in various tissues/stages are mentioned at the top with a colour scale, in which green, black and red denote low, medium and high levels of expression, respectively. Tissues/development stages of ICC 4958 and accession IDs of genes used for expression profiling are mentioned at the top and right-side of the expression map, respectively. FB: flower bud and FL: mature flower. (d) Differential expression profiling of a strong plant and SAM architectural trait-associated *CabHLH121* TF gene in the vegetative leaf, shoot and SAM tissues of two parental *desi* accessions (ICC 5590 and ICC 6306) of a RIL mapping population (ICC 5590 \times ICC 6306), as well as in two *kabuli* accessions (ICC 12968 and ICC 16814), contrasting with the plant architectural and SAM morphometric traits using the quantitative RT-PCR assay. Each bar denotes the mean (\pm standard error) of three independent biological replicates with two technical replicates for each sample used in the RT-PCR assay. *Significant difference in gene expression estimated by the LSD-ANOVA significance test at $P < 0.05$.

This exertion altogether identified four major genomic regions harbouring 18 major QTLs (6.0–16.8 logarithm of the odds, LOD) governing PW, PH, SWi, SH, and SA traits that were mapped on three chickpea chromosomes (*Ca04*, *Ca06* and *Ca08*) (Table S6, Figure S3). The PVE determined by individual QTLs for five studied architectural traits varied from 10.8 to 41.8% R^2 . The PVE estimated for all 18 QTLs in combination was 44.7% R^2 . The detected 18 major QTLs demonstrated additive effects for desirable PW, PH,

SWi, SH, and SA traits, reflecting the effective contribution of favourable alleles derived from both RIL mapping parental *desi* accessions ICC 5590 and ICC 6306 on these loci to modulate the plant and SAM architectural traits (Table S6).

The integration of QTL mapping with GWAS collectively demonstrated that non-synonymous coding SNPs in the four candidate genes linked to 18 major QTLs were significantly associated with PW, PH, SWi, SH, and SA traits (Tables 1 and S6 and Figures 3a,b and S3). Notably,

one non-synonymous SNP in a *CabHLH121* TF gene mapped on the major genomic region (1.360 cM corresponding to 281 622 bp) of *CaqPW/PH/SWi/SH/SA8.1* QTLs exhibited strong association potential for PW, PH, SWi, SH, and SA traits based on high-resolution GWAS (10^{-9} *P* with 34% PVE) and QTL mapping (11.8–16.8 LOD with 43.6% PVE) (Table 1, Table S6). At this major QTL region, an additive interaction was observed for QTLs/alleles governing desirable traits derived from both mapping parental *desi* accessions ICC 5590 and ICC 6306. In summary, informative non-synonymous SNP alleles of *CabHLH121* TF gene tightly linked to the major QTLs (*CaqPW/PH/SWi/SH/SA8.1*) governing PW, PH, SWi, SH, and SA traits were successfully validated by high-resolution GWAS, regional association analysis and QTL mapping in chickpea. Next, these functionally relevant molecular tags were selected as potential candidates for efficient dissection of plant architectural and SAM morphometric traits in chickpea.

Transcript profiling assures the regulatory function of a strong trait-associated *CabHLH121* TF gene for major plant architectural and SAM morphometric traits in chickpea

Four significant PW, PH, SWi, SH, and SA trait-associated genes, including a strong trait-associated *CabHLH121* TF validated by GWAS, regional association analysis and QTL mapping, were assessed for their differential regulatory function in controlling major plant architectural and SAM morphometric traits of chickpea. For this procedure, *in silico* global transcriptome profiling of said genes was performed in germinating seedlings, young leaves and SAM as well as four development stages of each immature flower bud and mature flower tissues of *desi* accession ICC 4958. All four trait-associated genes showed SAM-specific expression and were differentially upregulated (≥ 5 -fold at $P \leq 0.01$), especially in the SAM tissue, compared with germinating seedlings, young leaves, flower buds, and mature flowers of ICC 4958 (Figure 3c). Of these, a non-synonymous SNP-carrying *CabHLH121* TF gene associated strongly with PW, PH, SWi, SH, and SA traits and exhibiting pronounced SAM-specific expression was upregulated more than 12-fold in the SAM compared with the other analysed tissues of ICC 4958 (Figure 3c). Therefore, *CabHLH121* TF was considered a promising candidate gene regulating two major plant architectural traits (PW and PH), possibly through SAM proliferation and differentiation in chickpea.

To experimentally validate this strong trait-associated *CabHLH121* TF gene, its differential expression profiling was performed in the shoots, young leaves and SAM of two RIL mapping parental *desi* accessions (ICC 5590 and ICC 6306), as well as in two additional *kabuli* accessions (ICC 12968 and ICC 16814), contrasting with the PW, PH, SWi, SH, and SA traits assessed by quantitative RT-PCR

assay. The *CabHLH121* TF gene with a non-synonymous SNP showed SAM-specific expression and was significantly upregulated (15.2-fold) in the SAM compared with that in the respective shoots and young leaves of four said *desi* and *kabuli* accessions (Figure 3d). A pronounced upregulation (5.2-fold) of *CabHLH121* in the SAM of a broad PW/SWi and tall PH/SH *desi* mapping parental accession ICC 6306 with enhanced SAM morphometric characteristics was apparent compared with that of its counterpart narrow PW/SWi and dwarf PH/SH *desi* accession ICC 5590 (Figure 3d). However, only a 1.7-fold upregulation of *CabHLH121* was observed in broad PW/SWi and tall PH/SH *kabuli* accession ICC 16814 in comparison with its counterpart *kabuli* accession ICC 12968 with a narrow PW/SWi and dwarf PH/SH. When we compared the *desi* and *kabuli* accessions collectively, significant upregulated expression of *CabHLH121* was observed, especially in the SAM of a broad PW/SWi and tall PH/SH *desi* accession (ICC 6306) compared with a broad PW/SWi and tall PH/SH *kabuli* accession (ICC 16814) (Figure 3d). Overall, this finding infers that the degree of *CabHLH121* gene expression was enhanced significantly with the subsequent increase in PW, PH, SWi, SH, and SA, especially in the accessions of *desi* chickpea, suggesting a strong positive correlation between the gene expression level and varying plant/SAM architectural trait parameters.

Natural haplotypes of a *CabHLH121* TF gene govern major plant architectural and SAM morphometric traits in chickpea

A strong PW, PH, SWi, SH, and SA trait-associated *CabHLH121* TF gene showing SAM-specific upregulated expression, validated by GWAS, regional association analysis, QTL mapping and expression profiling, was sequenced among 291 *desi* and *kabuli* accessions (association panel) for molecular haplotyping. This task identified 35 SNPs, including 16 upstream regulatory SNPs as well as five missense and three non-sense non-synonymous and four synonymous coding SNPs, which altogether constituted two major haplotypes (HAP A and HAP B) (Figure 4a, b). The gene haplotype-based association analysis was performed by integrating the genotyping information for the SNP haplotypes in *CabHLH121* gene with multi-environment PW, PH, SWi, SH and SA trait phenotyping data among accessions of an association panel. This procedure revealed a strong association of haplotype HAP A (10^{-11} *P* with 36.7% PVE) with narrow PW (45–54 cm by 18 accessions)/dwarf PH (35–45 cm by 18 accessions)/narrow SWi (88–97 μm by 24 accessions)/dwarf SH (73–100 μm by 24 accessions)/less SA (6478–13 672 μm^2 by 26 accessions) traits, referred to here as DNDL (*desi* narrow PW/SWi, dwarf PH/SH, less SA). By contrast, haplotype HAP B (10^{-12} *P* with 38.5% PVE) exhibited a strong association with broad PW (55–69 cm by 56 accessions)/tall PH (46–66 cm by 56

accessions)/broad SWi (96–120 μm by 50 accessions)/tall SH (107–156 μm by 58 accessions)/high SA (14 270–18 569 μm^2 by 48 accessions) traits, hereafter referred to as DBTH (*desi* broad PW/SWi, tall PH/SH, high SA) (Figure 4c). In summary, the integrated genomic strategy involving molecular haplotyping and haplotype-specific association mapping delineated functionally relevant novel alleles and natural haplotypes (DNDL and DBTH) of *CabHLH121* TF gene regulating PW and PH traits by modulating the major SAM morphometric traits (SWi, SH and SA) in chickpea.

Fine-mapping and map-based cloning ascertains the role of a *CabHLH121* TF gene harbouring a major QTL in the regulation of vital plant architectural and SAM morphometric traits of chickpea

One strong 1.356 cM major QTL (*CaqPW/PH/SWi/SH/SA8.1*) interval (CaSNP8902(G/T) (1.058 cM) to CaSNP8909 (A/C) (2.414 cM)) harbouring a *CabHLH121* TF, mapped on chromosome 8 of a *desi* RIL genetic linkage map (ICC 5590 \times ICC 6306) was selected for fine-mapping to assure the potential of this gene in governing PW and PH traits of chickpea. For this process, a 1.356 cM genomic region corresponding to the indicated QTL interval (280.862 kb) from the parental accessions (ICC 5590 and ICC 6306) was introgressed and further backcrossed as recurrent and donor parents four times between each other to produce two BC₄F₄ NILs, DNDL-NIL^{*CaqPW/PH/SWi/SH/SA8.1*} and DBTH-NIL-*CaqPW/PH/SWi/SH/SA8.1* with approximately 81% recovery of the recurrent parental genome (Figure S6). Using 168 mapping individuals of a F₂ population (DNDL-NIL^{*CaqPW/PH/SWi/SH/SA8.1*} \times DBTH-NIL^{*CaqPW/PH/SWi/SH/SA8.1*}), 17 recombinants were detected between CaSNP8903(A/C) (1.206 cM) and CaSNP8908(A/T) (1.721 cM) SNPs at the 0.515 cM QTL interval (Figure 5a). This delineated genomic interval underlying *CaqPW/PH/SWi/SH/SA8.1* QTLs mapped on chromosome 8 was defined into the 106.641-kb region by integrating its genetic linkage map information with that of the physical map of the *kabuli* chickpea genome (Figure 5a).

The high-coverage (~117 \times) multiplex amplicon resequencing of a 106.641-kb QTL genomic region in the parental accessions and two selected DNDL and DBTH homozygous individuals of a mapping population (DNDL-NIL^{*CaqPW/PH/SWi/SH/SA8.1*} \times DBTH-NIL^{*CaqPW/PH/SWi/SH/SA8.1*}) together detected 605 SNPs with 18 protein-coding genes (Table S7). The QTL region-specific association analysis at a *CaqPW/PH/SWi/SH/SA8.1* QTL genomic interval was performed by integrating the genotyping information of 605 SNPs with the multienvironments (field/controlled condition) phenotyping data of the PW, PH, SWi, SH, and SA traits among 291 *desi* and *kabuli* accessions (association panel). This approach detected a strong plant and SAM architectural trait-associated *CabHLH121* TF gene mapped

in the 6.189-kb QTL genomic interval between CaS214(A/G) and CaS256(G/A) SNPs. High-resolution QTL mapping in the RILs as well as QTL-introgressed NILs and their integration with QTL region-specific association analysis overall scaled-down the 106.641-kb *CaqPW/PH/SWi/SH/SA8.1* QTL interval into a 6.189-kb genomic region (Figure 5b). By the comprehensive phenotyping of 17 recombinants following progeny testing, a 106.641-kb QTL genomic interval was resolved into the 6.189-kb region between CaS214(A/G) and CaS256(G/A) SNPs in seven selected most-promising recombinants of NILs (Figure 5b). The structural and functional annotation of this 6.189-kb QTL genomic interval with the *kabuli* genome identified one protein-coding gene, *CabHLH121* TF with accession ID *Ca_11909* (Figure 5b). A non-synonymous SNP (G/A) that was tightly linked to a *CabHLH121* TF and exhibiting zero recombination with this target locus in seven selected recombinants of NILs was considered the most-promising gene governing PW, PH, SWi, SH, and SA traits in chickpea. The same gene delineated through integrating high-resolution GWAS, regional association analysis and QTL mapping with molecular haplotyping and expression profiling was further validated by fine-mapping and map-based cloning in the RILs and NILs. Therefore, the *CabHLH121* TF gene harbouring a *CaqPW/PH/SWi/SH/SA8.1* major QTL indeed surfaced as the most potential candidate regulating PW and PH primarily by modulating major SAM morphometric traits (SWi, SH, and SA) in chickpea.

Development of NILs introgressed with superior *CabHLH121* gene haplotypes to understand their regulatory function in influencing major plant architectural and SAM morphometric traits of chickpea

For haplotype-assisted foreground selection, the SNPs flanking (CaS214(A/G) (277.582 kb) and CaS256(G/A) (283.771 kb)) and linked (CaKSNP3493(G/A) (281.622 kb)) to the 6.189-kb major *CaqPW/PH/SWi/SH/SA8.1* QTLs and the strong trait-associated *CabHLH121* TF gene haplotypes (DNDL and DBTH) were used (Figures 4d and S6). Subsequently, 10 positive lines screened by foreground selection were evaluated for background selection with the genome-wide 1536 parental (ICC 5590 and ICC 6306) polymorphic SNPs uniformly mapped on eight chromosomes. These procedures enhanced the recovery of the parental recurrent genome up to 97.2–98.0% in the constituted DNDL and DBTH gene (*CabHLH121* TF) haplotype-introgressed NILs, DNDL-NIL^{*CabHLH121(HAPA)*} and DBTH-NIL^{*CabHLH121(HAPB)*}. This result infers the efficacy of gene haplotype-assisted foreground/background selection compared with the most commonly used marker-assisted selection in the recovery of the parental recurrent genome as well as the precise selection of the most-promising recombinants for further genetic enhancement studies in chickpea.

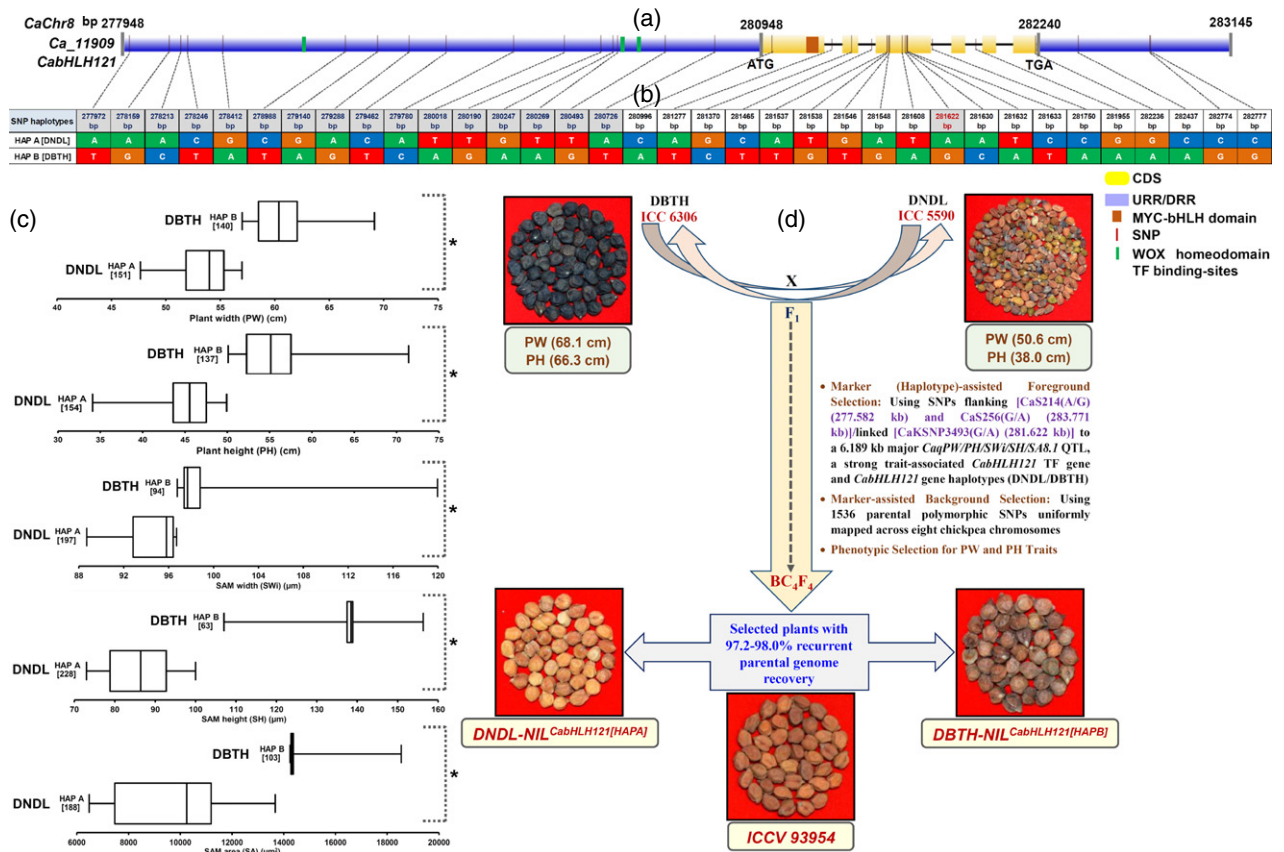


Figure 4. Molecular haplotyping of *CabHLH121* TF and development of gene haplotype-introgressed NILs.

(a, b) Genotyping of 35 SNPs mined from coding as well as non-coding introns and 3 kb of each URR and DRR sequence component of a *CabHLH121* TF gene among 291 *desi* and *kabuli* chickpea accessions (association panel) constituting two major haplotypes, HAP A (DNDL) and HAP B (DBTH). CDS: coding DNA sequence, URR/DRR: upstream/downstream regulatory region.

(c) Boxplots illustrating the significant phenotypic variation of five major plant architectural (PW and PH) and SAM morphometric (SWi, SH and SA) traits among 291 *desi* and *kabuli* chickpea accessions. Box edges denote the lower and upper quartiles, with median values shown in the middle of the box. Digits within the square parentheses indicate the number of *desi* and *kabuli* chickpea accessions represented by the individual haplotypes HAP A (DNDL) and HAP B (DBTH).

(d) Development of *CabHLH121* gene haplotype-introgressed NILs, DNDL-NIL^{*CabHLH121*(HAPA)} and DBTH-NIL^{*CabHLH121*(HAPB)} by marker (haplotype)-assisted foreground and background selection using two mapping parental accessions (ICC 5590 and ICC 6306), contrasting with the PW, PH, SWi, SH, and SA traits. These developed NILs were compared with a high-yielding Indian *desi* variety, ICCV 93954, to evaluate their overall agronomic performance, especially targeting five studied plant architectural and SAM morphometric traits in the field and controlled environment. DNDL: *Desi* narrow plant/SAM width, dwarf plant/SH, less SAM area. DBTH: *Desi* broad plant/SAM width, tall plant/SAM height, high SAM area.

The *CabHLH121* TF gene haplotype-specific differential expression profiling depicted a higher expression (≥ 6 -fold) and enhanced accumulation of transcript of the DNDL gene haplotype in the SAM of corresponding haplotype-introgressed NILs (DNDL-NIL^{*CabHLH121*(HAPA)}) (Figure 6a). However, their counterpart DBTH-introgressed NILs (DBTH-NIL^{*CabHLH121*(HAPB)}) had lower expression and a reduced transcript accumulation of the DBTH gene haplotype.

The efficiency of *CabHLH121* gene haplotypes (DNDL and DBTH) in modulating plant/SAM architectural traits was assured based on the comprehensive phenotypic evaluation and characterization of corresponding haplotype-introgressed NILs (DNDL-NIL^{*CabHLH121*(HAPA)} and DBTH-NIL^{*CabHLH121*(HAPB)}). For this process, SAM morphometric parameters, including SWi, SH, SA, SAL, SMWi, and SR, were measured in these NILs along with RIL

mapping parental *desi* accessions (ICC 5590 and ICC 6306) through histology. The results demonstrated high significant trait values of all these SAM morphometric features in the DBTH-NIL^{*CabHLH121*(HAPB)} line compared with those estimated in the DNDL-NIL^{*CabHLH121*(HAPA)} line (Figure 7a,b). The field phenotypic evaluation and scanning electron microscopy (SEM) of these NILs along with mapping parental accessions revealed that the DBTH-NIL^{*CabHLH121*(HAPB)} line with a broad PW and tall PH had a 1.7 to 2-fold higher SA compared with the DNDL-NIL^{*CabHLH121*(HAPA)} line with a narrow PW and dwarf PH (Figure 8a,b). A comprehensive correlation analysis and subsequent hierarchical cluster display demonstrated a significant positive correlation (88–94%) among SAM morphometric and plant architectural traits (PW, PH, SWi, SH, SA, SAL, and SR) in the developed NILs (Figure 7c).

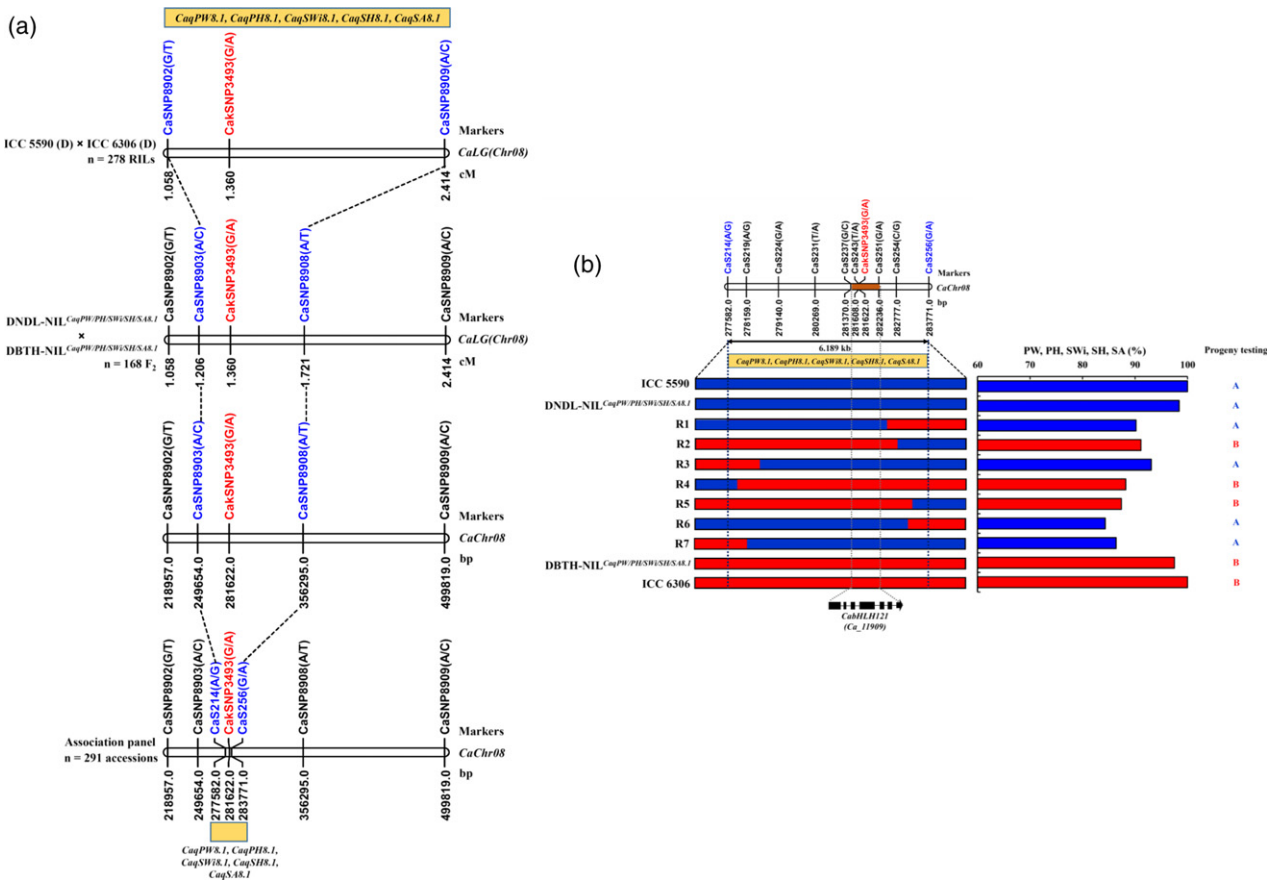


Figure 5. Fine-mapping and map-based cloning narrowed-down a major QTL into *CabHLH121* TF gene controlling major plant and SAM architectural traits in chickpea. (a) Map-based cloning of a major *CaqPW/PH/SWi/SH/SA8.1* QTL by fine-mapping in a NIL mapping population (DNDL-NIL^{*CaqPW/PH/SWi/SH/SA8.1*} × DBTH-NIL^{*CaqPW/PH/SWi/SH/SA8.1*}) and subsequent QTL region-specific association analysis in 291 *desi* and *kabuli* chickpea accessions contrasting with plant architectural and SAM morphometric traits (PW, PH, SWi, SH, and SA). The identity of the markers mapped on the linkage groups (LGs)/chromosomes and their genetic (cM)/physical (bp) positions are indicated above and below the chromosomes, respectively. The SNPs flanking and tightly linked to the QTLs governing the PW, PH, SWi, SH, and SA traits are indicated in blue and red colour, respectively. (b) Progeny testing-based individual phenotyping of seven selected recombinants as well as contrasting NILs (DNDL-NIL^{*CaqPW/PH/SWi/SH/SA8.1*} and DBTH-NIL^{*CaqPW/PH/SWi/SH/SA8.1*}) and mapping parental accessions (ICC 5590 and ICC 6306) to deduce the genotype of a 6.189-kb delineated major *CaqPW/PH/SWi/SH/SA8.1* QTL in chickpea. A non-synonymous SNP, CakSNP3493 (G/A), tightly linked to the *CabHLH121* TF gene and exhibiting zero recombination in seven selected recombinants was associated strongly with PW, PH, SWi, SH, and SA traits in chickpea. The genomic constitution of DNDL (*Desi* narrow plant/SAM width, dwarf plant/SAM height, less SAM area) and DBTH (*Desi* broad plant/SAM width, tall plant/SAM height, high SAM area) NILs/parental accessions are represented by ‘A’ and ‘B’, respectively.

The promoter of *CabHLH121* interacts with *CaWUS* TF, a master regulator of stem cell niche

The molecular basis of the differential expression of a strong trait-associated SAM-specific *CabHLH121* TF and its constituted DNDL and DBTH gene haplotypes in influencing major plant architectural (PW and PH) and SAM morphometric (SWi, SH, and SA) traits was determined. To achieve this goal, the 3-kb upstream regulatory region (URR) of a *CabHLH121* gene was scanned primarily for the presence of known *cis*-regulatory elements/TF binding sites. This procedure detected an abundance of AT-hook and GATA binding sequences comprising 14–21% of the total identified TF binding sites in the URR of a *CabHLH121* gene in chickpea (Figure S7). Interestingly, 5% of these mined known *cis*-regulatory element regions contained

WOX-homeodomain TF binding sites in the 3-kb URR of a *CabHLH121* gene. Comprehensive *in silico* analysis further demonstrated that a homeodomain TF gene (*Ca_01974*) encoding *WUSCHEL* (*CaWUS*) in chickpea, orthologous to the Arabidopsis *AtWUS* gene (*At2g17950*), potentially bound to these WOX-homeodomain TF binding sites in the URR (promoter) of *CabHLH121*. Therefore, this identified *CaWUS*, a master regulator of stem cell maintenance, proliferation and differentiation of SAM in multiple crop plants, may directly target and essentially regulate the expression of a *CabHLH121* TF gene in chickpea (Leiboff *et al.*, 2015; Thompson *et al.*, 2015; Lee *et al.*, 2016).

To ascertain the binding of *CaWUS* to the TF binding sites of the URR of *CabHLH121*, both chromatin immunoprecipitation (ChIP)-seq and ChIP-qPCR assays were

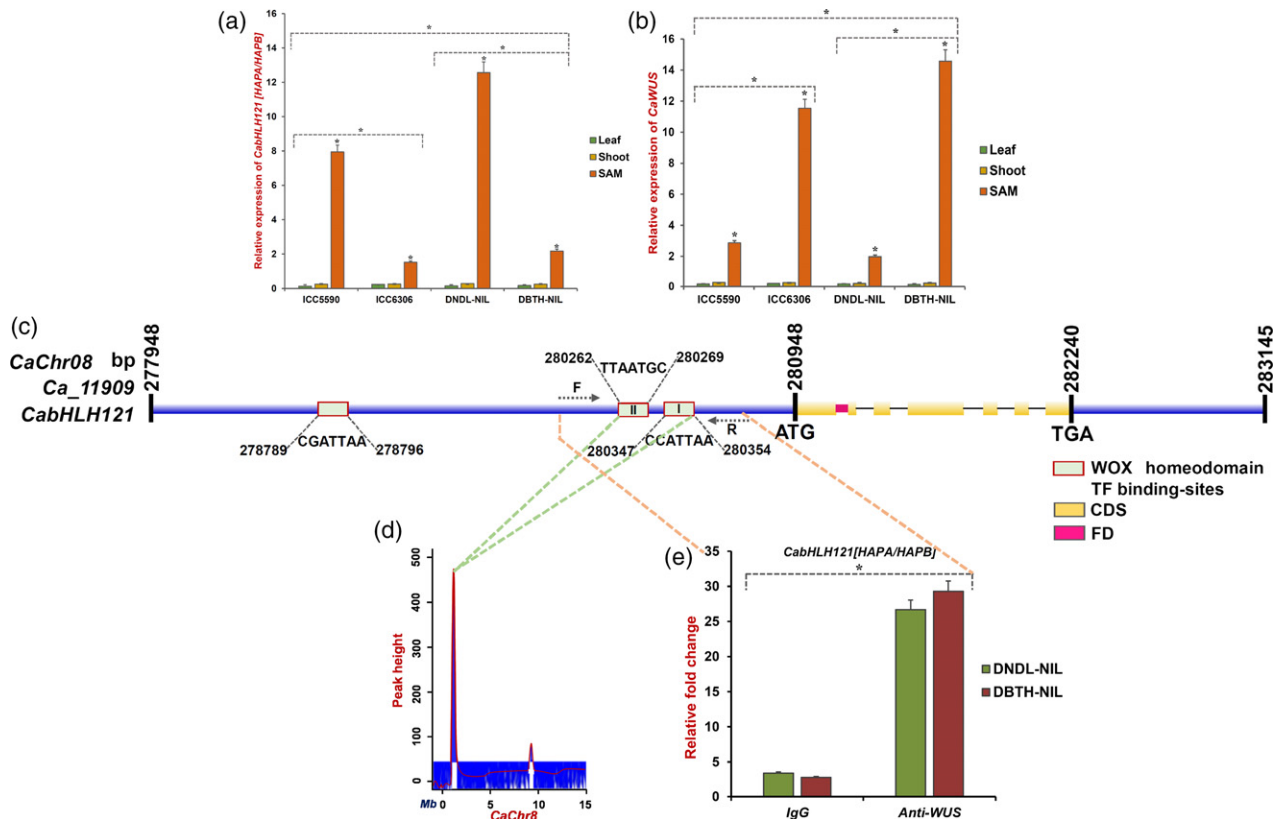


Figure 6. *CabHLH121* is transcriptionally regulated by *CaWUS*, a homeobox TF.

(a, b) Differential expression profiling of the delineated *CabHLH121* and *CaWUS* genes in the vegetative leaf, shoot and SAM tissues of two parental *desi* accessions (ICC 5590 and ICC 6306) of a RIL mapping population and developed NILs (DNDL-NIL and DBTH-NIL) using the quantitative RT-PCR assay. Each bar denotes the mean (\pm standard error) of three independent biological replicates with two technical replicates for each sample used in the RT-PCR assay. *Significant differences in gene expression measured by an LSD-ANOVA significance test at $P < 0.05$.

(c) Gene structural annotation illustrating the accurate position (bp) of binding of a *CaWUS* to the WOX-homeodomain TF binding sites in the 3-kb upstream regulatory (promoter) region of a *CabHLH121* TF gene, determined by DNA-protein interaction assays (ChIP-seq and ChIP-qPCR). CDS: coding DNA sequence and FD: functional domain.

(d, e) ChIP-seq was performed using the DNDL-NIL and DBTH-NIL lines by immunoprecipitation of the chromatin complex with an anti-*WUS* antibody and using immunoglobulin G (IgG) as a negative control, followed by sequencing of the immunoprecipitated DNA.

(d) ChIP-seq derived peak with a highest peak height of 267 revealed the binding of *CaWUS* to the concurrent WOX-homeodomain TF binding sites in the upstream regulatory (promoter) regions (280 262–280 269 bp and 280 347–280 354 bp) of the *CabHLH121* TF gene.

(e) The ChIP-qPCR assay confirmed the binding of *CaWUS* to the successive *WUS* TF binding sites in the aforesaid upstream regulatory region of the *CabHLH121* gene. ChIP-qPCR was performed to amplify the immunoprecipitated DNA with forward/reverse primers (indicated by arrows) targeting the *WUS* TF binding sites in *CabHLH121*. The ChIP-qPCR results are presented as fold changes by dividing the signals from ChIP with anti-*WUS* antibody by the IgG control. Bars denote the mean (\pm standard error). For a simpler representation, the *CabHLH121* gene haplotype-introgressed NILs, DNDL-NIL^{*CabHLH121*(HAPA)} and DBTH-NIL^{*CabHLH121*(HAPB)} are coded with DNDL-NIL and DBTH-NIL, respectively.

performed (Figure 6c–e). ChIP was performed in the DNDL-NIL^{*CabHLH121*(HAPA)} and DBTH-NIL^{*CabHLH121*(HAPB)} lines by immunoprecipitation of the chromatin complex with a *WUS*-specific antibody and IgG (immunoglobulin G) as a control. The sequencing of immunoprecipitated DNA and subsequent analysis of ChIP-seq data exhibited 17.8X genome coverage of the *kabuli* chickpea genome. Mapping of the sequence coverage at each physical position (bp) on the chickpea genome generated peaks with an abundant genomic distribution in the 3-kb regulatory region upstream of the translation initiation codon (ATG) of the *CabHLH121* gene. Genes in the URRs exhibiting similar peaks with a height < 90 in the control were removed, and the remaining 47 genes with a peak height ≥ 90 were

screened. The ChIP-seq outcome was further correlated with the known *cis*-regulatory element regions/TF binding sites predicted in the URR of a *CabHLH121* and its constituted DNDL and DBTH gene haplotypes (Figure 6c). This procedure identified *CaWUS* (*Ca_01974*) as a candidate TF with a maximum peak height of 267 that bound to the 594–686-bp region containing two predicted successive WOX-homeodomain TF binding sites in the URR of *CabHLH121* and both of its DNDL and DBTH gene haplotypes (Figure 6d). The structural annotation of these concurrent *WUS* TF binding sites in a *CabHLH121* gene revealed their correspondence to the 280262–280269 and 280347–280354-bp pseudomolecule sequence physical positions on chromosome 8. The ChIP-qPCR assay using the chromatin

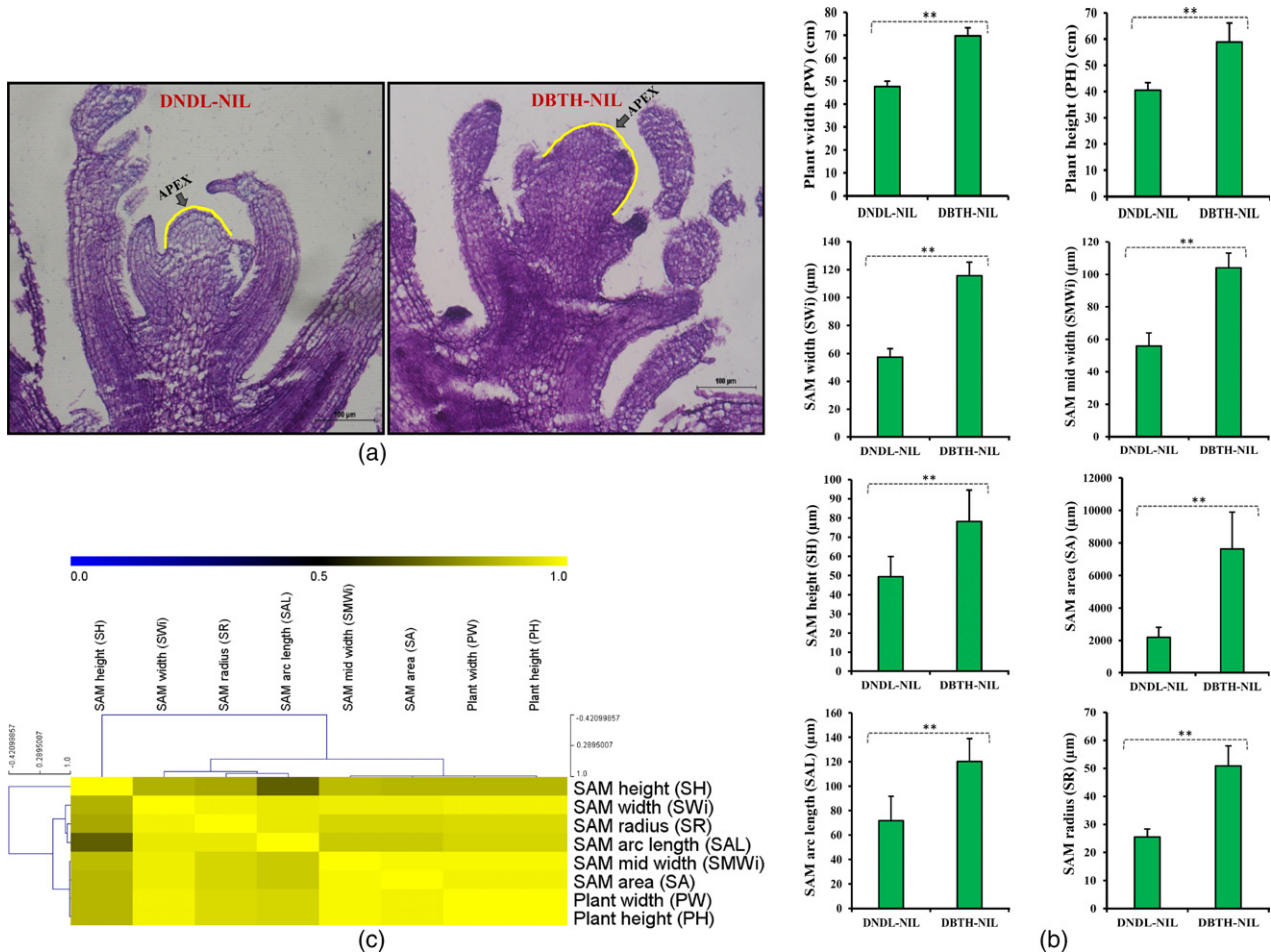


Figure 7. Phenotypic variation of major SAM morphometric and plant architectural traits in the developed NILs.

(a) SAM architecture of the DNDL-NIL and DBTH-NIL lines examined based on major morphometric trait parameters (SWi, SH, SMWi, SR, SAL and SA) using a histological assay, indicating their markedly altered SAM architecture.

(b) Bar diagrams illustrating the measurement of plant architectural and SAM morphometric traits between DNDL-NIL and DBTH-NIL lines. Dotted lines represent significant variation among DNDL-NIL and DBTH-NIL lines. Significance at a * $P < 0.05$ (pair-wise t-test) and ** $P < 0.01$ (pair-wise t-test). The *CabHLH121* gene haplotype-introgressed NILs, DNDL-NIL*CabHLH121*(HAPA) and DBTH-NIL*CabHLH121*(HAPB) are indicated by DNDL-NIL and DBTH-NIL, respectively.

(c) A hierarchical cluster display depicting the phenotypic correlation among major plant architectural (PW and PH) and SAM morphometric (SWi, SH, SMWi, SR, SAL and SA) traits in the NILs. The mean Pearson's correlation value estimated among the traits is represented at the top with a colour scale; blue, dark blue and yellow denote low, medium and high levels of correlation, respectively. Digits indicated in the vertical and horizontal bars illustrate the range (minimum, optimum and maximum) of correlation coefficient among the studied traits.

immunoprecipitated DNA from the DNDL-NIL^{*CabHLH121*} (HAPA) and DBTH-NIL^{*CabHLH121*}(HAPB) lines was performed with gene-specific primers. This process revealed the binding of a *CaWUS* to the *WOX*-homeodomain TF binding sites in the URR of a *CabHLH121* gene/haplotype (DNDL and DBTH) in controlling their transcriptional regulation for differential SAM morphometric characteristics and plant architectural traits of chickpea (Figure 6e). Furthermore, differential expression profiling of a *CaWUS* revealed lower expression (≥ 7 -fold) and a reduced accumulation of its transcript in the SAM of the DNDL-NIL^{*CabHLH121*}(HAPA) line (Figure 6b). However, their counterpart DBTH-NIL^{*CabHLH121*}(HAPB) line showed higher expression and enhanced accumulation of the *CaWUS* transcript.

Phenotypic evaluation and characterization of *CabHLH121* gene haplotypes-introgressed NILs for vital agronomic traits

The effects of the *CabHLH121* gene haplotypes (DNDL and DBTH) on major plant architectural and SAM morphometric traits were compared between NILs (DNDL-NIL^{*CabHLH121*}(HAPA) and DBTH-NIL^{*CabHLH121*}(HAPB)), along with RIL mapping parental *desi* accessions (ICC 5590 and ICC 6306) and a high-yielding Indian *desi* chickpea variety (ICCV 93954), based on their multienvironment replicated phenotypic evaluation in the field. Compared with the other lines, the DNDL-NIL^{*CabHLH121*}(HAPA) line exhibited an optimal PW (47.6 cm) and desirable semidwarf PH

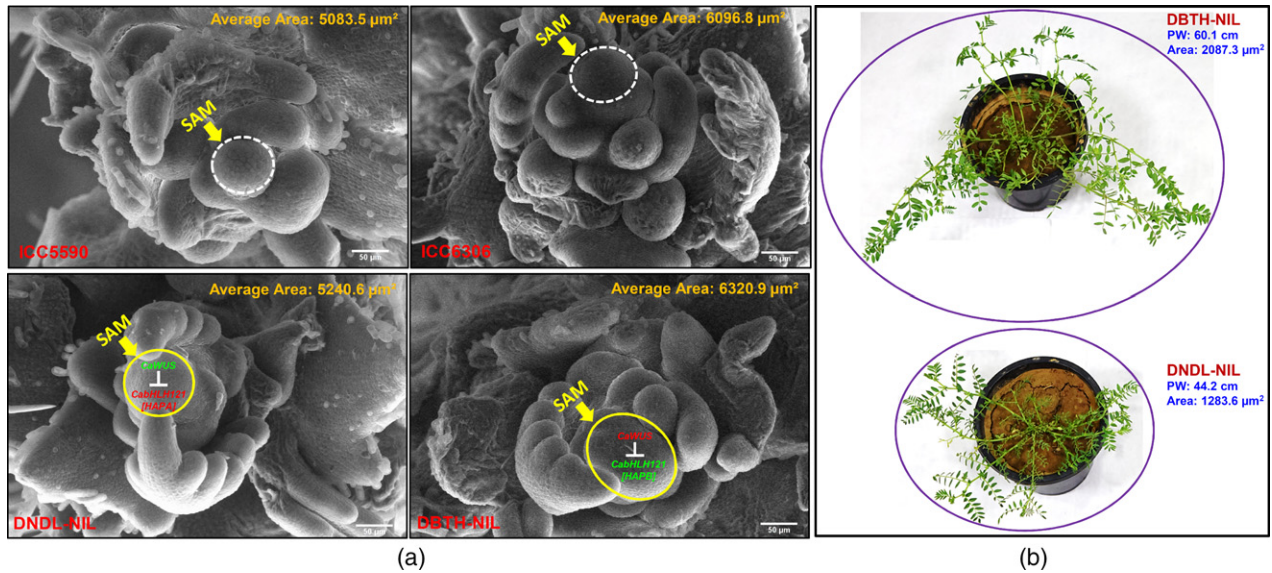


Figure 8. Correlation of PW with SAM morphometric parameters regulated by interplay between CabHLH121 and CaWUS.

(a) SAM architecture of two *desi* accessions (ICC 5590 and ICC 6306) of an RIL mapping population and two NIL lines (DNDL-NIL and DBTH-NIL) examined based on a major SAM morphometric parameter using SEM, revealing a marked variation in the average SAM area (μm^2) among these accessions/NILs. Comparative overview model depicting the role of a CaWUS in the differential transcriptional regulation and repression of the CabHLH121 TF gene, thereby modulating the average SAM area in the meristematic stem cell population of SAM representing the DNDL-NIL and DBTH-NIL lines. CaWUS and CabHLH121 are highlighted with green and red colour based on their downregulated and upregulated expression, respectively, in the DNDL-NIL and DBTH-NIL lines. (b) Replicated field phenotypic evaluation and characterization of DNDL-NIL and DBTH-NIL lines exhibiting striking differences in plant width (PW), as reflected by their significant variation in the average area (μm^2) under the curves. The CabHLH121 gene haplotype-introgressed NILs, DNDL-NIL^{CabHLH121(HAPA)} and DBTH-NIL^{CabHLH121(HAPB)} are marked by DNDL-NIL and DBTH-NIL, respectively.

(40.5 cm) without compromising its multiple other desirable plant architectures, agromorphological, and seed yield trait attributes. These useful agronomic trait characteristics included a semierect plant growth habit, yellow brown seed colour, and early flowering (48 days) and maturity (101 days) time, as well as an increased branch and pod/seed number and enhanced seed weight, yield per plant and yield per hectare (productivity), among others (Figure 4d, Table S8). The developed superior NILs (DNDL-NIL-CabHLH121(HAPA)) by contrast with the other analysed NILs and accessions together showed 26, 31.2, and 31.7% decreases in flowering/maturity time, PH and PW, respectively, with a 13.3% increase in yield/productivity. This finding implicates the greater efficacy of the superior DNDL haplotype delineated from a CabHLH121 TF gene in imparting optimal PW and PH without undesirable pleiotropic effects on other agromorphological and yield component traits. Henceforth, these functionally relevant molecular tags will be useful to develop high-yielding new plant type cultivars that are restructured with a desirable PH and PW through the modulation of vital plant architectural and SAM morphometric traits in chickpea.

DISCUSSION

Efficient genetic manipulation of various major plant architectural traits is vital to achieve enhanced yield and

productivity in crop plants (Pickersgill, 2007; Jin *et al.*, 2008; Wang and Li, 2008). Plant architectural traits, including PH and width, are modulated by differentiation, proliferation and maintenance of the meristematic stem cell population, which can be primarily assessed by quantitative measurements of diverse SAM morphometric trait parameters, such as SAM volume/size (height, width, and area), in crops (Thompson *et al.*, 2014, 2015; Leiboff *et al.*, 2015; Cai *et al.*, 2016; Saxena *et al.*, 2017). From this perspective, this study evaluated the multi-environment (field/controlled condition) phenotypic variation in two vital plant architectural traits (PW and PH) and correlated the findings with seven major SAM morphometric trait parameters (SH, SWi, SMWi, SH/SWi, SA, SAL, and SR) in the constituted association panel (291 *desi* and *kabuli* germplasm accessions) and RIL/NIL mapping individuals of chickpea through histological and SEM assays. A strong positive correlation (91–93%) of PW and PH with the SAM morphometric trait characteristics was evident among accessions/individuals, especially for *desi* chickpea. However, this observed definite correlation between SAM morphometric and plant architectural traits was not valid among accessions of *kabuli* chickpea, potentially due to distinct differences in the genetic backgrounds as well as striking variation in the agromorphological characteristics between *desi* and *kabuli* chickpea (Varshney *et al.*, 2013a,b;

Purushothaman *et al.*, 2014; Penmetsa *et al.*, 2016). The detailed phenotypic evaluation and characterization of large-scale natural and mapping populations collectively inferred that major SAM morphometric trait parameters, including SWi, SH, and SA, served as prime indicators to define and understand the genetic basis of the broad phenotypic variation observed for PW and PH traits, particularly among accessions of *desi* chickpea, and therefore can be targeted in genomics-assisted breeding for the genetic enhancement of chickpea. This finding further ascertains the direct involvement of SAM morphometric features in controlling the two major plant architectural traits (PW and PH), possibly by influencing the differentiation and proliferation of the meristematic stem cell population in the SAM of at least *desi* chickpea.

In this context, a comprehensive analysis of these plant architectural (PW and PH) and SAM morphometric traits was performed by integrating GWAS, regional association analysis, QTL/fine-mapping, map-based cloning, and molecular haplotyping with gene haplotype-specific association and transcript profiling, as well as the protein–DNA interaction assay, in the constituted association panel and mapping populations of chickpea. This procedure rapidly delineated natural allelic variants and haplotypes (DNDL and DBTH) of a *CabHLH121* TF gene within the major *CaqPW/PH/SWi/SH/SA8.1* QTL that regulates PW, PH, and SAM morphometric traits primarily through the proliferation and differentiation of the SAM meristematic stem cell population in *desi* chickpea. The identification of potential molecular tags of a single *CabHLH121* TF gene in imparting differential SAM morphometric characteristics and plant architectural traits owes to their strong phenotypic correlation in natural and mapping populations of chickpea.

The *CabHLH121* TF and its constituted gene haplotypes (DNDL and DBTH) is transcriptionally regulated by a master regulator, *CaWUS*, as evidenced by expression profiling and protein–DNA interaction assays (ChIP-seq and ChIP-qPCR) in the corresponding haplotype-introgressed NILs. The *WUS* and some other *WOX* family TFs are key players in maintaining the meristematic stem cell population in the model plant *Arabidopsis* as well as many other crop plants (Laux *et al.*, 1996; Leibfried *et al.*, 2005; Leiboff *et al.*, 2015; Thompson *et al.*, 2015; Lee *et al.*, 2016). *WUS* is known to bind, coordinate and repress the transcriptional activity of a *bHLH* TF gene, *HECATE1* (*HEC1*), and thereby essentially promote meristematic stem cell proliferation and SAM size expansion in crop plants (Buechel *et al.*, 2010; Schuster *et al.*, 2014; Sparks and Benfey, 2014). In this study, the delineated *bHLH* TF *CabHLH121* was found to be one of the major TFs regulating both PH and PW traits simultaneously in chickpea. *CabHLH121* acts downstream of a *CaWUS* in the signalling cascade and is responsible for the transcriptional regulation of major genes affecting SAM morphometric traits in chickpea. An inverse relationship

between the expression pattern of *CabHLH121* and *CaWUS* suggests a possible feedback loop in which an enhanced transcript level of *CabHLH121* in turn represses *CaWUS* transcription either directly or through TF intermediates.

A pronounced high expression level of *CaWUS* causes substantial transcriptional repression of the target *CabHLH121* gene/haplotype (DBTH) in the DBTH haplotype-introgressed NILs (DBTH-NIL^{*CabHLH121*(HAPB)}) and *desi* mapping parental accession (ICC 6306) with broad PW/SWi, tall PH/SH and high SA (Figure 8a). This finding is apparent based on a downregulation that includes a reduced expression and accumulation of *CabHLH121* transcripts, thereby promoting enhanced proliferation of the meristematic stem cell population and enlargement of the SAM in the corresponding haplotype-introgressed NILs. By contrast, DNDL haplotype-introgressed NILs (DNDL-NIL-*CabHLH121*(HAPA)) and the *desi* RIL mapping parental accession (ICC 5590) with a narrow PW/SWi, dwarf PH/SH and less SA exhibited reduced expression of a *CaWUS*, causing minimal/optimal transcriptional repression of the target *CabHLH121* gene/haplotype (DNDL), as evidenced by its upregulation, including the enhanced expression and accumulation of transcripts. These salient findings implicate the essentiality of the effective binding and transcriptional regulation (repression) of *CaWUS* and its target *CabHLH121* gene/haplotypes for the modulation of various plant and SAM architectural traits (narrow versus broad PW/SWi and dwarf versus tall PH/SH) in chickpea.

Therefore, superior transcriptional signatures (natural alleles and haplotypes) delineated from the *CabHLH121* TF gene using a genome-wide integrated genomic strategy are efficacious for the regulation of a desirable optimal PW and semidwarf PH via modulating SAM morphometric traits in chickpea. As a consequence, a *CabHLH121* TF and its DNDL and DBTH gene haplotypes regulating SAM morphometric trait characteristics can be genetically manipulated to achieve desirable plant architectural traits that will be useful to develop ideal plant type cultivars restructured with optimal PW and PH (semidwarf) in chickpea. This phenomenon was evident from the NILs (DNDL-NIL^{*CabHLH121*(HAPA)}) introgressed with a superior *CabHLH121* gene haplotype (DNDL), which exhibited an optimal PW and semidwarf PH without any undesirable pleiotropic effects on other agromorphological and yield component traits. The new plant type cultivars restructured with the desirable plant architecture of optimal PW and PH therefore showed proficiency in enhancing yield and productivity in chickpea.

Chickpea requires a recommended planting density of 30 (row × row) and 10 (plant × plant) cm of spacing for uniform growth, development and maximum yield; therefore, at most, 330 000 plants of diverse accessions can be planted per hectare of field area for cultivation. By contrast, we were able to accommodate 450 000 plants of the developed superior NILs (DNDL-NIL^{*CabHLH121*(HAPA)}) with an

optimal PW (47.6 cm) and desirable PH (semidwarf with 40.5 cm PH) per hectare of cultivable field area at a planting density of 25 (row × row) and 5 (plant × plant) cm of spacing, without compromising the yield per plant and other agronomic traits. The observed 13% higher yield/productivity in the superior DNDL-NIL^{CabHLH121(HAPA)} line was not due to an enhanced yield per plant, however, because of their dense plant population with a 25% increase in planting density versus that recommended for chickpea per hectare of cultivable field area. The efficient, rapid and integrated genomic strategy employed in this study has potential for the development of a superior *CabHLH121* gene haplotype-introgressed *desi* chickpea line that produces a high yield and productivity by restructuring the plant architectural (desirable PW and PH) and SAM morphometric traits. This achievement will essentially provide better remuneration to farmers with rational land use, therefore ensuring global food security in the present context of an increasing population density and declining per capita land area.

EXPERIMENTAL PROCEDURES

Plant materials

An association panel for PW and PH was constituted by screening 291 diverse chickpea germplasm accessions, including 189 *desi* and 102 *kabuli* (Table S1), from the available core collection for association mapping (Kujur *et al.*, 2015a). The association panel included two of each cultivated *desi* (ICC 5590 and ICC 6306) and *kabuli* (ICC 12968 and ICC 16814) accessions with contrasting PW and PH traits. ICC 5590, a traditional cultivar (landrace) originating from India, is a narrow and dwarf *desi* accession with a PW and PH of 50.6 and 38.0 cm, respectively. ICC 6306, a landrace originating from the Russian Federation, is a broad and tall *desi* accession with a PW and PH of 68.1 and 66.3 cm, respectively. ICC 12968, a released variety from India, is a narrow and semidwarf *kabuli* accession with a PW and PH of 52.2 and 45.9 cm, respectively. ICC 16814, a landrace originating from Portugal, is a broad and tall *kabuli* accession with a PW and PH of 64.3 and 57.3 cm, respectively. ICC 5590 and ICC 6306 were inter-crossed with each other to develop a *desi* 278 F₇ RIL mapping population (ICC 5590 × ICC 6306) for QTL mapping.

Field phenotyping

The germplasm accessions and mapping individuals belonging to an association panel and RIL population, respectively, were grown and phenotyped in the experimental field for two successive years (2013 and 2014) during the normal crop season as per the randomized complete block design (RCBD) with two replications. These procedures were performed in two geographical regions, Hyderabad (latitude 17°3'N/longitude 77°2'E from October to February) and New Delhi (28°4'N/77°2'E from November to March), following standard agronomic practices. The PW and PH traits were measured by estimating the mean canopy height (cm) and spread (cm), respectively, of 10 representative plants belonging to each accession and the RIL from the soil surface at the time of the flower-ending and pod-setting-initiation stage. Genetic inheritance characteristics, such as the frequency distribution, CV, and broad-sense H², of traits among accessions and RILs were determined according to Bajaj *et al.* (2015b).

Plant growth conditions

To optimize the appropriate timing for collecting the SAM and assessing their major morphometric trait variations, the seeds of each germplasm accession and RIL mapping individual were planted in pots filled with the 2:1:1 mixture of field soil: soilrite: manure, respectively. Plants were grown in the controlled growth chamber under 10-h day light and 14-h night dark conditions between 20 and 22°C temperatures with 60% relative humidity. For SAM histology, 30 plants of each accession and RIL were grown for 10–12 days after germination. SAM samples from 10-day-old seedlings (exhibiting normal and uniform growth) of each accession and RIL that attained full vegetative size, but not showing signs of any transition from the vegetative to the reproductive phase, were collected with at least three biological replicates to study their histology and major morphometric trait variation.

Histological assay

To perform histology including fixation, dehydration, paraplast embedding, and block preparation of SAM tissues, the shoot apices of each accession and RIL were collected individually and processed in accordance with Gautam *et al.* (2016) and Ranjan *et al.* (2017). Tissue blocks of the appropriate size and orientation were sectioned using a rotary microtome (Leica Biosystems, USA) to obtain strips of 8- to 10-μm-thick sections, which were flattened by floating for 1–2 min at 50–55°C. Flattened tissue sections were mounted on charged slides and dried at 42°C overnight to attach the tissues on the slide surface. A light microscope (Leedz Micro Imaging Limited, UK) along with Zeiss AxioVision were used to capture and visualize the SAM images. At least three independent biological replicates with three technical replicates for each accession and RIL were used for histology of SAM and the study of their major morphometric trait variations.

SAM morphometric measurements

The SAM architecture of each accession and RIL were measured by seven major morphometric trait parameters, including the SWi, SH, SMWi, SH/SWi, SAL, SA, and SR using ImageJ 1.31 v (<http://rsb.info.nih.gov/ij/>), with three biological and technical replicates (Schindelin *et al.*, 2015). SWi was measured from the notch of P1 to P2 clefts, whereas SH was estimated from the apex of the SAM to the width line at the base (Figure 1a). SMWi was calculated at the midpoint of the SH, while SAL was measured by tracing the outer distance from the SAM apex to the P1 cleft. SA was measured using the ImageJ freehand selection tool, and SR was calculated from the emergence point of the P1 cleft to the centre of SWi (Figure 1a).

Large-scale discovery and genotyping of genome-wide SNPs

A 96-plex GBS library was constructed using the genomic DNA of 291 *desi* and *kabuli* chickpea accessions belonging to an association panel. This included two accessions representing *desi* (ICC 5590 and ICC 6306) and *kabuli* (ICC 12968 and ICC 16814) with contrasting PW and PH traits. The GBS library was sequenced with an Illumina HiSeq2000 (Illumina Inc., USA) next-generation sequencing (NGS) platform, and further high-quality sequences were demultiplexed according to Kujur *et al.* (2015a,b,c). The generated sequences were mapped on the *kabuli* genome (Varshney *et al.*, 2013b; <http://gigadb.org/dataset/100076>) following Kujur *et al.* (2015a,b,c). Non-erroneous SNPs were discovered and structurally/functionally annotated on the diverse coding and non-

coding sequence components of *kabuli* genes and genomes (chromosomes/pseudomolecules and unanchored scaffolds) using customized Perl scripts, the single nucleotide polymorphism effect predictor (SnpEff v3.1h; <http://snpeff.sourceforge.net>) and PFAM database v27.0 (<http://pfam.sanger.ac.uk>) according to Kujur *et al.* (2015a,b,c) and Srivastava *et al.* (2017). The genomic distribution of SNPs in accordance with their physical positions (bp) on eight chromosome pseudomolecules of *kabuli* genome was visualized with a Circos (Krzywinski *et al.*, 2009).

Molecular diversity and linkage disequilibrium decay

To study the molecular diversity, the genome-wide SNP genotyping data generated among 291 *desi* and *kabuli* chickpea accessions (association panel) were analysed with PowerMarker (Liu and Muse, 2005), STRUCTURE v2.3.4 (Pritchard *et al.*, 2000) and MEGA7 (Kumar *et al.*, 2016). Accordingly, an unrooted neighbour-joining (NJ) phylogenetic tree was constructed among accessions based on Nei's diversity coefficient (Nei *et al.*, 1983) with 1000 bootstrap replicates. The population genetic structure among accessions was determined according to Kujur *et al.* (2015a,c).

To estimate the genome-wide LD decay, the genotyping data for SNPs physically mapped on chromosomes were analysed with PLINK (Purcell *et al.*, 2007) and TASSEL (Bradbury *et al.*, 2007; <http://www.maizegenetics.net>) following Zhao *et al.* (2011) and Kujur *et al.* (2015a). The genome-wide LD decay was determined by plotting the average r^2 (frequency correlation among pair of alleles across a pair of SNP loci) measured from the population (defined by population genetic structure) of a constituted association panel against the 50-kb uniform physical interval across eight chromosomes.

Genome-wide association study

The population structure (Q), PCA (P), and kinship (K)-matrix were estimated using STRUCTURE, GAPIT (Lipka *et al.*, 2012) and SPAGeDi 1.2 (Hardy and Vekemans, 2002), respectively. To perform GWAS, the SNP genotyping, phenotyping, and molecular diversity information generated from an association panel were analysed with the GLM and MLM approaches of TASSEL as well as the CMLM ((P + K), K and Q + K) (Zhang *et al.*, 2010; Kang *et al.*, 2010)), population parameters previously determined (P3D) and the efficient mixed model association eXpedited (EMMAX) interface of GAPIT (Lipka *et al.*, 2012), according to Kujur *et al.* (2015a) and Upadhyaya *et al.* (2015). To assure the accuracy of SNP marker-trait association, a quantile-quantile (Q-Q) plot-based Benjamini-Hochberg FDR cut-off ≤ 0.05 (Benjamini and Hochberg, 1995) correction for multiple comparisons between observed/expected $-\log_{10}(P)$ -values and an adjusted P -value threshold of significance was employed. Based on these procedures, SNP loci that were significantly associated with the traits at a lowest FDR adjusted P -value (threshold $P < 10^{-8}$) and highest R^2 were identified. The magnitude (R^2) of PVE by the traits was measured using an FDR-controlling model method with the SNP (adjusted P -value).

Regional association analysis and molecular haplotyping

The selected trait-associated genomic/gene regions were sequenced using the genomic DNA of 291 *desi* and *kabuli* chickpea accessions (association panel) by employing the multiplexed amplicon sequencing protocol (per the manufacturer's instructions) of TruSeq Custom Amplicon v1.5 in the Illumina MiSeq NGS platform according to Saxena *et al.* (2014a). The custom oligo probes targeting the selected genomic regions including

CDS (coding DNA sequences)/exons and introns as well as 3-kb of each URR and DRR (downstream regulatory regions) of the genes were designed using Illumina Design Studio and synthesized further for use in the targeted multiplexed amplicon sequencing. The pooling of amplicons (average size of 500 bp per reaction) into the custom amplicon tubes, construction of template libraries, normalization of uniquely tagged pooled amplicon libraries and sequencing of generated clusters by the Illumina MiSeq platform, were performed according to Saxena *et al.* (2014a) and Malik *et al.* (2016). The mapping of high-quality amplicon sequence reads onto the *kabuli* chickpea genome (Varshney *et al.*, 2013b), detection of high-quality SNPs among accessions and their structural/functional annotation on the *kabuli* genome were performed following Kujur *et al.* (2015a,c). The constitution of SNP haplotypes, determination of the SNP haplotype-based LD pattern and estimation of the association potential of haplotypes with the traits were performed according to Saxena *et al.* (2014a) and Kujur *et al.* (2015a,b).

High-resolution QTL mapping

The GBS-derived genome-wide SNP detecting polymorphisms between two contrasting parental accessions were genotyped using the genomic DNA of 278 mapping individuals of a *desi* RIL population (ICC 5590 \times ICC 6306) by the Sequenom MALDI-TOF MassARRAY assay (<http://www.sequenom.com>) according to Saxena *et al.* (2014a,b). The Kosambi mapping function interface of JoinMap 4.1 (www.kyazma.nl/index.php/mc.JoinMap) at a higher LOD threshold (≥ 4.0) was used to assign and map the SNPs into defined linkage groups (LG1 to LG8) based on their cM genetic distances and respective marker physical positions (bp) on the chromosomes (Kujur *et al.*, 2015a,c). Accordingly, a high-resolution genetic linkage map was constructed and visualized with MapChart v2.2 (Voorrips, 2002).

For QTL mapping, a significant CIM (composite interval mapping) function of MapQTL 6 (van Ooijen, 2009) at a LOD cut-off score > 5.0 with 1000 permutations at a $P < 0.05$ was used according to Bajaj *et al.* (2015a,b) and Kujur *et al.* (2015a,b). Accordingly, the PVE (%) and additive effect (evaluated by parental origin of favourable alleles) specified by each major QTL on traits at a significant LOD were determined according to Bajaj *et al.* (2015a,b). The confidence interval (CI) of each significant major QTL peak was evaluated using ± 1 -LOD support intervals (95% CI).

Fine-mapping and map-based cloning

A major QTL region identified by high-resolution QTL mapping (ICC 5590 \times ICC 6306) in an RIL population was targeted for fine-mapping. This procedure was performed by developing two BC₄F₄ NILs according to the strategies depicted in Figure S6. One BC₄F₄ NIL was developed as a DNDL (*desi* narrow PW/SWi, dwarf PH/SH, and low SA)-NIL^{CaqPW/PH/SWi/SH/SA8.1}. Another BC₄F₄ NIL was developed as a DBTH (*desi* broad PW/SWi, tall PH/SH, and high SA)-NIL^{CaqPW/PH/SWi/SH/SA8.1}. The generated NILs were inter-crossed among each other to develop a F₂ mapping population (DNDL-NIL \times DBTH-NIL) consisting of 168 individuals. SNPs showing parental polymorphisms between ICC 5590 and ICC 6306 at this QTL genomic interval were genotyped in 168 mapping individuals using the MALDI-TOF assay according to Saxena *et al.* (2014a,b). Field and controlled environment phenotyping of mapping individuals for the traits and QTL mapping were performed according to the aforesaid strategies. For the QTL region-specific association analysis, a target QTL genomic interval was sequenced using the genomic DNA of the parental accessions (ICC 5590 and ICC 6306) and two selected homozygous individuals of a mapping

population (DNDL-NIL × DBTH-NIL) that contrasted with the studied traits. The sequencing and mapping of high-quality amplicon sequence reads as well as the detection of SNPs and their structural/functional annotation onto the *kabuli* genome were performed following Saxena *et al.* (2014a,b), Kujur *et al.* (2015a,c) and Malik *et al.* (2016). The genotyping of SNPs mined at a major QTL genomic interval among accessions, phenotyping and trait association analysis were performed following the aforesaid methods. For progeny analysis, homozygous recombinant and homozygous non-recombinant individuals derived from the NILs with contrasting traits were selected based on their genetic constitution and considering the recombination among SNPs flanking/tightly linked to a major QTL, as well as a strong trait-associated gene and its constituted DNDL and DBTH haplotypes. The selected recombinant and non-recombinant progenies were phenotyped for the studied traits. Significant variations of traits between selected recombinant and non-recombinant progenies were evaluated by a statistical one-tailed *t*-test.

For marker (haplotype)-assisted foreground selection, SNPs flanking/tightly linked to a major QTL as well as a strong trait-associated gene and its DNDL and DBTH haplotypes were genotyped among individuals of the back-cross mapping population using the MALDI-TOF assay following Saxena *et al.* (2014a,b). For marker (haplotype)-assisted background selection, 1536 SNPs showing polymorphisms between parental accessions (ICC 5590 and ICC 6306) of an RIL mapping population (ICC 5590 × ICC 6306) and that mapped uniformly across the chromosomes of the *kabuli* genome were genotyped in the selected back-cross mapping individuals by the Illumina GoldenGate SNP genotyping assay according to Bajaj *et al.* (2015a) (Figure S6). Large-scale mapping individuals of the back-cross population were phenotyped for the traits in the field as well as in the controlled growth conditions with at least three replications, according to the aforementioned methods. The NILs introgressed with the DNDL and DBTH haplotypes were further phenotyped for the SWi, SH and SA traits following the described histological assay.

Scanning electron microscopy

For the SEM assay, 10-day-old SAM tissues of RIL mapping parental accessions (ICC 5590 and ICC 6306) as well as DNDL and DBTH gene haplotype-introgressed NILs were fixed in FAA (3.7% formaldehyde, 50% ethanol and 5% acetic acid) solution and treated overnight with 0.2% osmium tetroxide followed by serial ethanol dehydration according to Kujur *et al.* (2015a) and Ranjan *et al.* (2017). The dehydrated samples were further processed by critical-point drying and examined by SEM (Evo LS25; Zeiss). All the SEM-captured images of SAM were processed with ImageJ to measure their major morphometric parameters and variations among accessions and NILs.

Differential expression profiling

For *in silico* global expression profiling of the trait-associated genes, the raw FASTAQ transcriptome sequence data of germinating seedlings, young leaves, SAM, and eight different development stages of flower buds/flowers of a *desi* chickpea accession ICC 4958 were acquired from the NCBI-SRA (sequence read archive) database (Singh *et al.*, 2013), and the high-quality sequences were mapped on the *kabuli* genome. Global transcriptome profiling was performed according to Srivastava *et al.* (2016). The expression profiles of trait-associated chickpea genes were retrieved, analysed and visualized with a heat map using the MultiExperiment Viewer (MeV, <http://www.tm4.org/mev>).

For experimental validation, RIL mapping parental accessions (ICC 5590 and ICC 6306) and *kabuli* accessions (ICC 12968 and ICC 16814), as well as DNDL and DBTH gene haplotype-introgressed NILs, were grown in the controlled environment according to the aforementioned strategy. High-quality RNA was isolated from the shoot, leaf and SAM tissues of 10-day-grown plants of the described accessions/NILs with biological and technical replicates. Quantitative real-time (RT)-PCR was performed by amplifying the isolated RNA with specific primers designed based on the gene/haplotype and an internal control gene, *Actin*, following Bajaj *et al.* (2015b) and Upadhyaya *et al.* (2015). The $2^{-\Delta\Delta CT}$ method and two-tailed *t*-test were employed to determine the expression pattern of the gene/haplotypes and their significant differences in expression, respectively, among accessions/NILs (Bajaj *et al.*, 2015b; Mukhopadhyay and Tyagi, 2015). The expression profile was visualized with a heat map using MeV (<http://www.tm4.org/mev>).

Identification and analysis of *cis*-regulatory elements

The sequence of the 3-kb URR of a strong trait-associated gene was acquired based on the respective genomic coordinates and structural annotation of the *kabuli* genome. The obtained URR sequence was further analysed in PlantPAN 2.0 (<http://plantpan2.itps.ncku.edu.tw/>) to scan for the presence of *cis*-regulatory elements or known TF-binding sites. These known TF-binding sites of a trait-associated gene were correlated with the SNPs and haplotypes identified based on the URR of a target gene among 291 *desi* and *kabuli* chickpea accessions (association panel), as well as the aforesaid *in silico* and experimental differential expression profile of the gene/haplotypes.

ChIP (chromatin immunoprecipitation) assay

For the ChIP analysis, the SAM of 10-day-old plants of individual NILs introgressed with DNDL and DBTH gene haplotypes were used to isolate nuclei to immunoprecipitate the sonicated chromatin suspension with the protein–DNA complex using a TF gene-specific antibody (Roche, USA) as previously described (Sun *et al.*, 2015; Tian *et al.*, 2017). The antibody was specific to a TF gene that was predicted to bind in the TF-binding site (*cis*-regulatory element region) of the URR of a strong trait-associated gene. Three biological/technical replicates representing individual haplotypes along with immunoglobulin G (IgG) as a control were assayed in the ChIP experiment. For ChIP sequencing (ChIP-seq), libraries were prepared from chromatin immunoprecipitated DNA and sequenced using an Illumina HiSeq4000 (Illumina Inc., USA) NGS platform according to the manufacturer's instructions. Quality checking of the sequences and mapping of high-quality sequences on the *kabuli* genome were performed according to Kujur *et al.* (2015a,c). The ChIP-enriched peaks were identified based on the sequence coverage at individual physical positions (bp) on the *kabuli* genome (Varshney *et al.*, 2013b) following Sun *et al.* (2015). The ChIP-quantitative PCR (ChIP-qPCR) assay was performed by amplifying the equally quantified said chromatin immunoprecipitated DNA isolated from the NILs with gene/haplotype-specific primers. Primer pairs were designed targeting the ChIP-seq validated TF-binding sites identified in the URR of a strong trait-associated gene following the aforementioned RT-PCR methods. The outcomes of both ChIP-seq and ChIP-PCR assays were ascertained by three independent sequencing and PCR experiments using three biological/technical replicates.

ACKNOWLEDGEMENTS

We are very much grateful to Mr Sube Singh, lead scientific officer, Grain Legumes Research Program/GenBank, ICRISAT, Hyderabad for assisting in collecting the multienvironments field

phenotyping data for the germplasm accessions and mapping population. Constant assistance was provided by all the scientific and technical staff from NIPGR and IARI, New Delhi, India and ICRISAT, Hyderabad to conduct this research study is acknowledged. We are also thankful to the central instrumentation facility (CIF), the plant growth facility (PGF) and the DBT-eLibrary Consortium (DeLCON) of NIPGR, New Delhi for providing timely support and access to e-resources for this research work.

FUNDING

The financial support for this study was provided by a research grant from the Department of Biotechnology (DBT), Government of India. LN, UB, VT, and AD acknowledge the UGC (University Grants Commission) and DBT, India for research fellowship awards.

CONFLICT OF INTEREST

The authors declare that they have no conflicts of interest.

AUTHORS CONTRIBUTIONS

LN, UB, DB, NM, and VT performed the field and laboratory experiments as well as drafted the manuscript. ST, VSH, and HDU helped in constitution/generation of association panel and mapping populations and performed field phenotyping. AD, DB, and AS helped in the large-scale SNP genotyping data analyses. AKS, AKT, and SKP conceived and designed the research study, guided data analysis and interpretation, participated in drafting and correcting the manuscript critically. All authors gave the final approval of the version to be published.

SUPPORTING INFORMATION

Additional Supporting Information may be found in the online version of this article.

Figure S1. Genomic distribution and structural annotation of 333001 SNPs physically mapped on eight chromosomes and unanchored scaffolds of *kabuli* genome.

Figure S2. Determination of molecular diversity, phylogenetic relationship and historical recombination (linkage disequilibrium) among 291 *desi* (189) and *kabuli* (102) germplasm accessions belonging to an association panel of chickpea.

Figure S3. Construction of a high-density genetic linkage map and molecular mapping of major QTLs governing vital plant architectural and SAM morphometric traits in chickpea.

Figure S4. Frequency distribution and boxplots depicting the phenotypic variation of major plant architectural and SAM morphometric traits in a RIL mapping population (ICC 5590 × ICC 6306).

Figure S5. A hierarchical cluster display depicting phenotypic correlation among five major plant architectural and SAM morphometric traits in 278 mapping individuals of a RIL population (ICC 5590 × ICC 6306).

Figure S6. Schematic illustration of the comprehensive strategies followed to develop NILs of chickpea by marker (haplotype)-assisted foreground and background selection.

Figure S7. Relative proportion of known *cis*-regulatory elements/transcription factor (TF) binding sites predicted in a 3 kb regulatory (promoter) sequence upstream to the translation initiation codon (ATG) of *CabHLH121*.

Table S1. Germplasm accessions utilized for dissection of major plant architectural and SAM morphometric traits in chickpea.

Table S2. Genetic inheritance pattern of traits in the association panel and RIL mapping population used for GWAS and QTL mapping.

Table S3. Genome-wide SNPs mined for GWAS of major plant architectural and SAM morphometric traits in chickpea.

Table S4. SNPs employed to construct a high-density genetic linkage map (ICC 5590 × ICC 6306) of chickpea.

Table S5. Genome-wide SNPs mapped on eight chromosomes of a chickpea genetic linkage map.

Table S6. Molecular mapping of major QTLs governing five major plant architectural and SAM morphometric traits in chickpea.

Table S7. SNPs mined within a major QTL interval for QTL region-specific association analysis in chickpea.

Table S8. Comparative assessment of agronomic trait characteristics between haplotype-introgressed NILs *vis-à-vis* mapping parental accessions and a high-yielding Indian variety of chickpea.

Data S1. Results.

REFERENCES

- Bajaj, D., Upadhyaya, H.D., Khan, Y. *et al.* (2015a) A combinatorial approach of comprehensive QTL-based comparative genome mapping and transcript profiling identified a seed weight-regulating candidate gene in chickpea. *Sci. Rep.* **5**, 9264.
- Bajaj, D., Saxena, M.S., Kujur, A. *et al.* (2015b) Genome-wide conserved non-coding microsatellite (CNMS) marker-based integrative genetical genomics for quantitative dissection of seed weight in chickpea. *J. Exp. Bot.* **66**, 1271–1290.
- Barton, M.K. (2010) Twenty years on: the inner workings of the shoot apical meristem, a developmental dynamo. *Dev. Biol.* **341**, 95–113.
- Benjamini, Y. and Hochberg, Y. (1995) Controlling the false discovery rate: a practical and powerful approach to multiple testing. *J. R. Stat. Soc. Series B Stat. Methodol.* **57**, 289–300.
- Bradbury, P.J., Zhang, Z., Kroon, D.E., Casstevens, T.M., Ramdoss, Y. and Buckler, E.S. (2007) TASSEL: Software for association mapping of complex traits in diverse samples. *Bioinformatics*, **23**, 2633–2635.
- Buechel, S., Leibfried, A., To, J.P., Zhao, Z., Andersen, S.U., Kieber, J.J. and Lohmann, J.U. (2010) Role of A-type *ARABIDOPSIS* RESPONSE REGULATORS in meristem maintenance and regeneration. *Eur. J. Cell Biol.* **89**, 279–284.
- Cai, G., Yang, Q., Chen, H., Yang, Q., Zhang, C., Fan, C. and Zhou, Y. (2016) Genetic dissection of plant architecture and yield-related traits in *Brassica napus*. *Sci. Rep.* **6**, 21625.
- Evenson, R.E. and Gollin, D. (2003) Assessing the impact of the green revolution, 1960 to 2000. *Science*, **300**, 758–762.
- Gautam, V., Singh, A., Singh, S. and Sarkar, A.K. (2016) An efficient LCM-based method for tissue specific expression analysis of genes and miRNAs. *Sci. Rep.* **6**, 21577.
- Gupta, S., Nawaz, K., Parween, S., Roy, R., Sahu, K., Kumar Pole, A., Khandal, H., Srivastava, R., Kumar Parida, S. and Chattopadhyay, D. (2016) Draft genome sequence of *Cicer reticulatum* L., the wild progenitor of chickpea provides a resource for agronomic trait improvement. *DNA Res.* **24**, 1–10.
- Hardy, O.J. and Vekemans, X. (2002) SPAGeDi: a versatile computer program to analyse spatial genetic structure at the individual or population levels. *Mol. Ecol. Notes*, **2**, 618–620.
- Jain, M., Misra, G., Patel, R.K. *et al.* (2013) A draft genome sequence of the pulse crop chickpea (*Cicer arietinum* L.). *Plant J.* **74**, 715–729.
- Jin, J., Huang, W., Gao, J.P., Yang, J., Shi, M., Zhu, M.Z., Luo, D. and Lin, H.X. (2008) Genetic control of rice plant architecture under domestication. *Nat. Genet.* **40**, 1365–1369.
- Kang, H.M., Sul, J.H., Service, S.K., Zaitlen, N.A., Kong, S.Y., Freimer, N.B., Sabatti, C. and Eskin, E. (2010) Variance component model to account for sample structure in genome-wide association studies. *Nat. Genet.* **42**, 348–354.

- Krzywinski, M., Schein, J., Birol, I., Connors, J., Gascoyne, R., Horsman, D., Jones, S.J. and Marra, M.A. (2009) Circos: an information aesthetic for comparative genomics. *Genome Res.* **19**, 1639–1645.
- Kujur, A., Bajaj, D., Upadhyaya, H.D. *et al.* (2015a) A genome-wide SNP scan accelerates trait-regulatory genomic loci identification in chickpea. *Sci. Rep.* **5**, 11166.
- Kujur, A., Upadhyaya, H.D., Shree, T. *et al.* (2015b) Ultra-high density intra-specific genetic linkage maps accelerate identification of functionally relevant molecular tags governing important agronomic traits in chickpea. *Sci. Rep.* **5**, 9468.
- Kujur, A., Bajaj, D., Upadhyaya, H.D. *et al.* (2015c) Employing genome-wide SNP discovery and genotyping strategy to extrapolate the natural allelic diversity and domestication patterns in chickpea. *Front. Plant Sci.* **6**, 162.
- Kujur, A., Upadhyaya, H.D., Bajaj, D., Gowda, C.L., Sharma, S., Tyagi, A.K. and Parida, S.K. (2016) Identification of candidate genes and natural allelic variants for QTLs governing plant height in chickpea. *Sci. Rep.* **6**, 27968.
- Kumar, J., Choudhary, A.K., Solanki, R.K. and Pratap, A. (2011) Towards marker-assisted selection in pulses: a review. *Plant Breed.* **130**, 297–313.
- Kumar, S., Stecher, G. and Tamura, K. (2016) MEGA7: Molecular evolutionary genetics analysis version 7.0 for bigger datasets. *Mol. Biol. Evol.* **33**, 1870–1874.
- Laux, T., Mayer, K.F., Berger, J. and Jürgens, G. (1996) The *WUSCHEL* gene is required for shoot and floral meristem integrity in *Arabidopsis*. *Development*, **122**, 87–96.
- Lee, D.K., Parrott, D.L., Adhikari, E., Fraser, N. and Sieburth, L.E. (2016) The mobile bypass signal arrests shoot growth by disrupting shoot apical meristem maintenance, cytokinin signaling, and WUS transcription factor expression. *Plant Physiol.* **171**, 2178–2190.
- Leibfried, A., To, J.P., Busch, W., Stehling, S., Kehle, A., Demar, M., Kieber, J.J. and Lohmann, J.U. (2005) *WUSCHEL* controls meristem function by direct regulation of cytokinin-inducible response regulators. *Nature*, **438**, 1172–1175.
- Leiboff, S., Li, X., Hu, H.C. *et al.* (2015) Genetic control of morphometric diversity in the maize shoot apical meristem. *Nat. Commun.* **6**, 8974.
- Lipka, A.E., Tian, F., Wang, Q., Peiffer, J., Li, M., Bradbury, P.J., Gore, M.A., Buckler, E.S. and Zhang, Z. (2012) GAPIT: genome association and prediction integrated tool. *Bioinformatics*, **2**, 2397–2399.
- Liu, K. and Muse, S.V. (2005) PowerMarker: an integrated analysis environment for genetic marker analysis. *Bioinformatics*, **21**, 2128–2129.
- Malik, N., Dwivedi, N., Singh, A.K., Parida, S.K., Agarwal, P., Thakur, J.K. and Tyagi, A.K. (2016) An integrated genomic strategy delineates candidate mediator genes regulating grain size and weight in rice. *Sci. Rep.* **6**, 23253.
- Mukhopadhyay, P. and Tyagi, A.K. (2015) *OsTCP19* influences developmental and abiotic stress signaling by modulating ABI4-mediated pathways. *Sci. Rep.* **5**, 9998.
- Nei, M., Tajima, F. and Tateno, Y. (1983) Accuracy of estimated phylogenetic trees from molecular data. II. Gene frequency data. *J. Mol. Evol.* **19**, 153–170.
- van Ooijen, J.W. (2009) *MapQTL 6, Software for the Mapping of Quantitative Trait Loci in Experimental Populations of Diploid Species*. Wageningen, Netherlands: Kyazma BV.
- Parween, S., Nawaz, K., Roy, R. *et al.* (2015) An advanced draft genome assembly of a *desi* type chickpea (*Cicer arietinum* L.). *Sci. Rep.* **5**, 12806.
- Peng, J., Richards, D.E., Hartley, N.M. *et al.* (1999) Green revolution genes encode mutant gibberellin response modulators. *Nature*, **400**, 256–261.
- Penmetsa, V.R., Carrasquilla-Garcia, N., Bergmann, E.M. *et al.* (2016) Multiple post-domestication origins of *kabuli* chickpea through allelic variation in a diversification-associated transcription factor. *New Phytol.* **211**, 1440–1451.
- Pickersgill, B. (2007) Domestication of plants in the Americas: insights from Mendelian and molecular genetics. *Ann. Bot.* **100**, 925–940.
- Pritchard, J.K., Stephens, M. and Donnelly, P. (2000) Inference of population structure using multilocus genotype data. *Genetics*, **155**, 945–959.
- Purcell, S., Neale, B., Todd-Brown, K. *et al.* (2007) PLINK: a tool set for whole-genome association and population-based linkage analyses. *Am. J. Hum. Genet.* **81**, 559–575.
- Purushothaman, R., Upadhyaya, H.D., Gaur, P.M., Gowda, C.L.L. and Krishnamurthy, L. (2014) *Kabuli* and *desi* chickpeas differ in their requirement for reproductive duration. *Field Crops Res.* **163**, 24–31.
- Ranjan, R., Khurana, R., Malik, N., Badoni, S., Parida, S.K., Kapoor, S. and Tyagi, A.K. (2017) *bHLH142* regulates various metabolic pathway-related genes to affect pollen development and anther dehiscence in rice. *Sci. Rep.* **7**, 43397.
- Reinhardt, D. and Kuhlemeier, C. (2002) Plant architecture. *EMBO Rep.* **3**, 846–851.
- Sakamoto, T., Miura, K., Itoh, H. *et al.* (2004) An overview of gibberellin metabolism enzyme genes and their related mutants in rice. *Plant Physiol.* **134**, 1642–1653.
- Saxena, M.S., Bajaj, D., Das, S., Kujur, A., Kumar, V., Singh, M., Bansal, K.C., Tyagi, A.K. and Parida, S.K. (2014a) An integrated genomic approach for rapid delineation of candidate genes regulating agro-morphological traits in chickpea. *DNA Res.* **21**, 695–710.
- Saxena, M.S., Bajaj, D., Kujur, A., Das, S., Badoni, S., Kumar, V., Singh, M., Bansal, K.C., Tyagi, A.K. and Parida, S.K. (2014b) Natural allelic diversity, genetic structure and linkage disequilibrium pattern in wild chickpea. *PLoS ONE*, **9**, e107484.
- Saxena, R.K., Obala, J., Sinjushin, A., Kumar, C.V.S., Saxena, K.B. and Varshney, R.K. (2017) Characterization and mapping of *Dt1* locus which co-segregates with *CcTFL1* for growth habit in pigeonpea. *Theor. Appl. Genet.* **130**, 1773–1784.
- Schindelin, J., Rueden, C.T., Hiner, M.C. and Eliceiri, K.W. (2015) The ImageJ ecosystem: an open platform for biomedical image analysis. *Mol. Reprod. Dev.* **82**, 518–529.
- Schuster, C., Gaillouchet, C., Medzihradsky, A., Busch, W., Daum, G., Krebs, M., Kehle, A. and Lohmann, J.U. (2014) A regulatory framework for shoot stem cell control integrating metabolic, transcriptional, and phytohormone signals. *Dev. Cell*, **28**, 438–449.
- Singh, V.K., Garg, R. and Jain, M. (2013) A global view of transcriptome dynamics during flower development in chickpea by deep sequencing. *Plant Biotechnol. J.* **11**, 691–701.
- Sparks, E.E. and Benfey, P.N. (2014) HEC of a job regulating stem cells. *Dev. Cell*, **28**, 349–350.
- Srivastava, R., Bajaj, D., Malik, A., Singh, M. and Parida, S.K. (2016) Transcriptome landscape of perennial wild *Cicer microphyllum* uncovers functionally relevant molecular tags regulating agronomic traits in chickpea. *Sci. Rep.* **6**, 33616.
- Srivastava, R., Upadhyaya, H.D., Kumar, R., Daware, A., Basu, U., Shimray, P.W., Tripathi, S., Bharadwaj, C., Tyagi, A.K. and Parida, S.K. (2017) A multiple QTL-Seq strategy delineates potential genomic loci governing flowering time in chickpea. *Front. Plant Sci.* **8**, 1105.
- Sun, T., Zhang, Y., Li, Y., Zhang, Q., Ding, Y. and Zhang, Y. (2015) ChIP-seq reveals broad roles of SARD1 and CBP60 g in regulating plant immunity. *Nat. Commun.* **6**, 10159.
- Thompson, A.M., Crants, J., Schnable, P.S., Yu, J., Timmermans, M.C., Springer, N.M., Scanlon, M.J. and Muehlbauer, G.J. (2014) Genetic control of maize shoot apical meristem architecture. *G3*, **4**, 1327–1337.
- Thompson, A.M., Yu, J., Timmermans, M.C., Schnable, P., Crants, J.C., Scanlon, M.J. and Muehlbauer, G.J. (2015) Diversity of maize shoot apical meristem architecture and its relationship to plant morphology. *G3*, **5**, 819–827.
- Tian, H., Wang, X., Guo, H., Cheng, Y., Hou, C., Chen, J.G. and Wang, S. (2017) NTL8 regulates trichome formation in *Arabidopsis* by directly activating R3 MYB genes *TRY* and *TCL1*. *Plant Physiol.* **174**, 2363–2375.
- Upadhyaya, H.D., Bajaj, D., Das, S. *et al.* (2015) A genome-scale integrated approach aids in genetic dissection of complex flowering time trait in chickpea. *Plant Mol. Biol.* **89**, 403–420.
- Varshney, R.K., Mohan, S.M., Gaur, P.M. *et al.* (2013a) Achievements and prospects of genomics-assisted breeding in three legume crops of the semiarid tropics. *Biotech. Adv.* **31**, 1120–1134.
- Varshney, R.K., Song, C., Saxena, R.K. *et al.* (2013b) Draft genome sequence of chickpea (*Cicer arietinum*) provides a resource for trait improvement. *Nat. Biotechnol.* **31**, 240–246.
- Voorrips, R.E. (2002) MapChart: Software for the graphical presentation of linkage maps and QTLs. *J. Hered.* **93**, 77–78.
- Wang, Y. and Li, J. (2008) Molecular basis of plant architecture. *Annu. Rev. Plant Biol.* **59**, 253–279.
- Yang, X.C. and Hwa, C.M. (2008) Genetic modification of plant architecture and variety improvement in rice. *Heredity*, **101**, 396–404.
- Yano, K., Yamamoto, E., Aya, K. *et al.* (2016) Genome-wide association study using whole-genome sequencing rapidly identifies new genes influencing agronomic traits in rice. *Nat. Genet.* **48**, 927–934.
- Zhang, Z., Ersoz, E., Lai, C.Q. *et al.* (2010) Mixed linear model approach adapted for genome-wide association studies. *Nat. Genet.* **42**, 355–360.
- Zhao, K., Tung, C.W., Eizenga, G.C. *et al.* (2011) Genome-wide association mapping reveals a rich genetic architecture of complex traits in *Oryza sativa*. *Nat. Commun.* **2**, 467.